Cell Biology
Developmental Biology

Female-germline specific protein Sakura interacts with Otu and is crucial for germline stem cell renewal and differentiation and oogenesis

Reviewed Preprint
v1 • November 27, 2024
Not revised

Azali Azlan, Li Zhu, Ryuya Fukunaga

Department of Biological Chemistry, Johns Hopkins School of Medicine, Baltimore, United States

eLife Assessment

This **valuable** study reports the first characterization of the CG14545 gene in Drosophila melanogaster, which the authors name "Sakura." Acting during germline stem cell fate and differentiation, Sakura is required for both oogenesis and female fertility. The evidence supporting the claims of the authors is **solid**, but the manuscript would be strengthened by a more in-depth investigation into the cause-and-effect relationships for the different defects observed.

https://doi.org/10.7554/eLife.103828.1.sa3

Abstract

During oogenesis, self-renewal and differentiation of germline stem cells (GSCs) must be tightly regulated. The *Drosophila* female germline serves as an excellent model for studying these regulatory mechanisms. Here, we report that a previously uncharacterized gene *CG14545*, which we named *sakura*, is essential for oogenesis and female fertility in *Drosophila*. Sakura is predominantly expressed in the ovaries, particularly in the germline cells, including GSCs. *sakura* null mutant female flies display rudimentary ovaries with germline-less and tumorous phenotypes, fail to produce eggs, and are completely sterile. The germline-specific depletion of *sakura* impairs Dpp/BMP signaling, leading to aberrant *bag-of-marbles* (*bam*) expression, resulting in faulty differentiation and loss of GSCs. Additionally, *sakura* is necessary for normal piwi-interacting RNAs (piRNAs) levels and for proper localization of Oo18 RNA-binding protein (Orb) in developing oocytes. We identified Ovarian Tumor (Otu) as protein binding partner of Sakura, and we found that loss of *otu* phenocopies loss of *sakura* in ovaries. Thus, we identified Sakura as a crucial factor for GSC renewal and differentiation and oogenesis, and propose that Sakura and Otu function together in these processes.

Introduction

Oogenesis is a complex process in which germline stem cells (GSCs) develop into mature female gametes or oocytes. This process involves multiple layers of regulations and numerous genes, some of which remain to be discovered and characterized. *Drosophila melanogaster*, a genetically tractable model organism, has long been at the forefront of oogenesis research.

Adult *Drosophila* females possess a pair of ovaries, each composed of 12-16 ovarioles. At the anterior tip of each ovariole is a structure called the germarium, which houses two to three GSCs (**Fig S1**). GSCs reside in the most anterior region of the germarium, where they directly contact cap cells and escort cells, forming a niche crucial for GSC self-renewal [1–3]. GSCs undergo asymmetric mitotic division, producing two distinct cells: one GSC and one cystoblast[1,4]. The cystoblast, destined to differentiate, undergoes four mitotic divisions with incomplete cytokinesis, resulting in interconnected cysts of 2, 4, 8, and 16 cells [5,6]. Of the 16 cells, one will differentiate into an oocyte, while the remaining 15 develop into polyploid nurse cells, which synthesize proteins and RNAs for deposition into the oocyte[7].

GSC proliferation is essential for proper oogenesis. GSCs must be tightly regulated to maintain their undifferentiated state while continuing to divide and differentiate. Failure in GSC self-renewal or inappropriate differentiation leads to stem cell loss, disrupting oocyte production[8,9]. Conversely, uncontrolled GSC division or defective differentiation results in an overabundance of GSC-like cells (a tumorous phenotype) and fewer differentiated cells, ultimately inhibiting oocyte production[10,11]. Thus, a precise balance between GSC self-renewal and cyst differentiation within the germarium is essential for proper oogenesis and is tightly regulated.

Bone Morphogenetic Protein (BMP) signaling plays a critical role in regulating GSC self-renewal and differentiation during *Drosophila* oogenesis. In the stem cell niche, GSCs are physically anchored to cap cells via adherens and gap junctions[12,13]. Cap cells secrete BMP ligands, such as Decapentaplegic (Dpp) and Glass bottom boat (Gbb), which are recognized by transducing receptors like Thickvein (Tkv) and Saxophone (Sax) on the GSCs[14,15] (**Fig S1**). Upon activation, these receptors phosphorylate a transcription factor Mad. The phosphorylated Mad (pMad) translocates into the nucleus, where it represses the transcription of *bag-of-marbles* (*bam*), a key differentiation factor [16,17].

Bam, a ubiquitin-associated protein, is essential for cystoblast differentiation. Dpp/BMP signaling in the niche represses *bam* expression, preventing GSCs from differentiating and enabling self-renew. However, as the daughter cells (cytoblasts) exit the niche, they derepress *bam* and initiate the differentiation program (**Fig S1**)[7]. Tight regulation of Dpp/BMP signaling and *bam* expression ensures that only cells within the niche adopt GSC fate, while adjacent daughter cells differentiate into cystoblasts. Loss of *bam* leads to blocked differentiation and the accumulation of GSC-like cells, whereas ectopic *bam* expression forces GSCs differentiation, depleting the stem cell pool [18–20].

One of the proteins that interacts with Bam is Ovarian Tumor (Otu). Otu forms a deubiquitinase complex with Bam, which deubiquitinates Cyclin A (CycA), stabilizing CycA and promoting GSC differentiation[21]. Otu is crucial for oogenesis and female fertility[22,23]. Mutations in the *otu* gene cause various ovarian defects, including tumorous growths, germ cell loss, and abnormalities in oocyte determination and nurse cell dumping, indicating Otu's importance in multiple stages of oogenesis[22–25]. However, the precise molecular mechanisms by which Otu functions in these processes remain largely unknown.

In this study, we aimed to identify a novel gene required for oogenesis. Through a search for uncharacterized genes expressed exclusively in *Drosophila* ovaries, we discovered *CG14545*, a gene encoding a 114 amino acids (aa) long protein without any known functional domain (**Fig 1A**). CG14545 is expressed specifically in female germline cells, including GSCs. Our genetic analysis revealed that *CG14545* is required for oogenesis and female fertility and plays an important intrinsic role in regulating GSCs renewal and differentiation. Additionally, CG14545 is important for the piRNA pathway. We identified Otu as a binding partner of the CG14545 protein, suggesting that both proteins may participate in the same molecular pathways to regulate GSC fate and differentiation. We named the *CG14545* gene *sakura*, meaning "cherry blossom" in Japanese, symbolizing birth and renewal.

Results

Sakura is exclusively expressed in the ovaries

Based on high-throughput expression data in Flybase, *sakura* mRNA is highly and exclusively expressed in adult ovaries (**Fig 1B**). To investigate Sakura protein expression, we generated a polyclonal anti-Sakura antibody against a recombinant full-length Sakura protein. Using this antibody, we examine Sakura protein expression at different stages of *Drosophila* development and across tissues. We found that Sakura protein is specifically expressed in the ovary, particularly in stage 1-11 oocytes (**Fig 1C**).

sakura mutant flies

To explore the biological and molecular functions of Sakura *in vivo*, we generated a *sakura* mutant allele ($sakura^{null}$) with a one nucleotide (nt) insertion replacing 33 nts within the Sakura coding region using the CRISPR/Cas9 genome editing system (**Fig 1A**)[26]. This mutation causes a frameshift and a premature stop codon, resulting in a 33-amino acid (aa) N-terminal fragment of Sakura followed by a 22-aa segment produced by frameshifted translation (**Fig 1A**). This truncated fragment is unlikely to be functional, and we were unable to detect stable protein expression, as shown below. Thus, we consider this allele a null mutation. $sakura^{null/null}$ flies were viable, revealing that Sakura is not essential for survival.

To validate the $sakura^{null}$ strain, we performed Western blots using ovary lysates from *sakura* mutant flies using the anti-Sakura antibody. As expected, full-length Sakura protein was detected in the ovaries of wild-type ($sakura^{+/+}$) and heterozygous controls ($sakura^{null/+}$), but not in those of homozygous mutants ($sakura^{null/null}$) (**Fig 1D**). No smaller protein corresponding to the truncated Sakura fragment was detected in either $sakura^{null/+}$ or $sakura^{null/null}$ ovaries thus, suggesting that the fragment is unstable or not expressed.

Sakura is cytoplasmic and expressed specifically in germ cells

To determine the localization of Sakura protein within the ovaries, we generated transgenic flies carrying a *sakura* coding sequence fused with EGFP at the C-terminus (*sakura*-EGFP) under the control of the *sakura* promoter. Western blot analysis of ovary lysates showed that Sakura-EGFP is expressed at levels comparable to endogenous Sakura (**Fig 1D**). Confocal imaging revealed that Sakura-EGFP is specifically expressed in the cytoplasm of germ cells, including GSCs, cyst cells, nurse cells, and developing oocytes (**Fig 1E** and **1F**). Sakura-EGFP was not expressed in somatic cells such as terminal filament, cap cells, escort cells, or follicle cells. (**Fig 1E**). In the egg chamber, Sakura-EGFP was detected in the cytoplasm of nurse cells and was enriched in developing oocytes (**Fig 1F**).

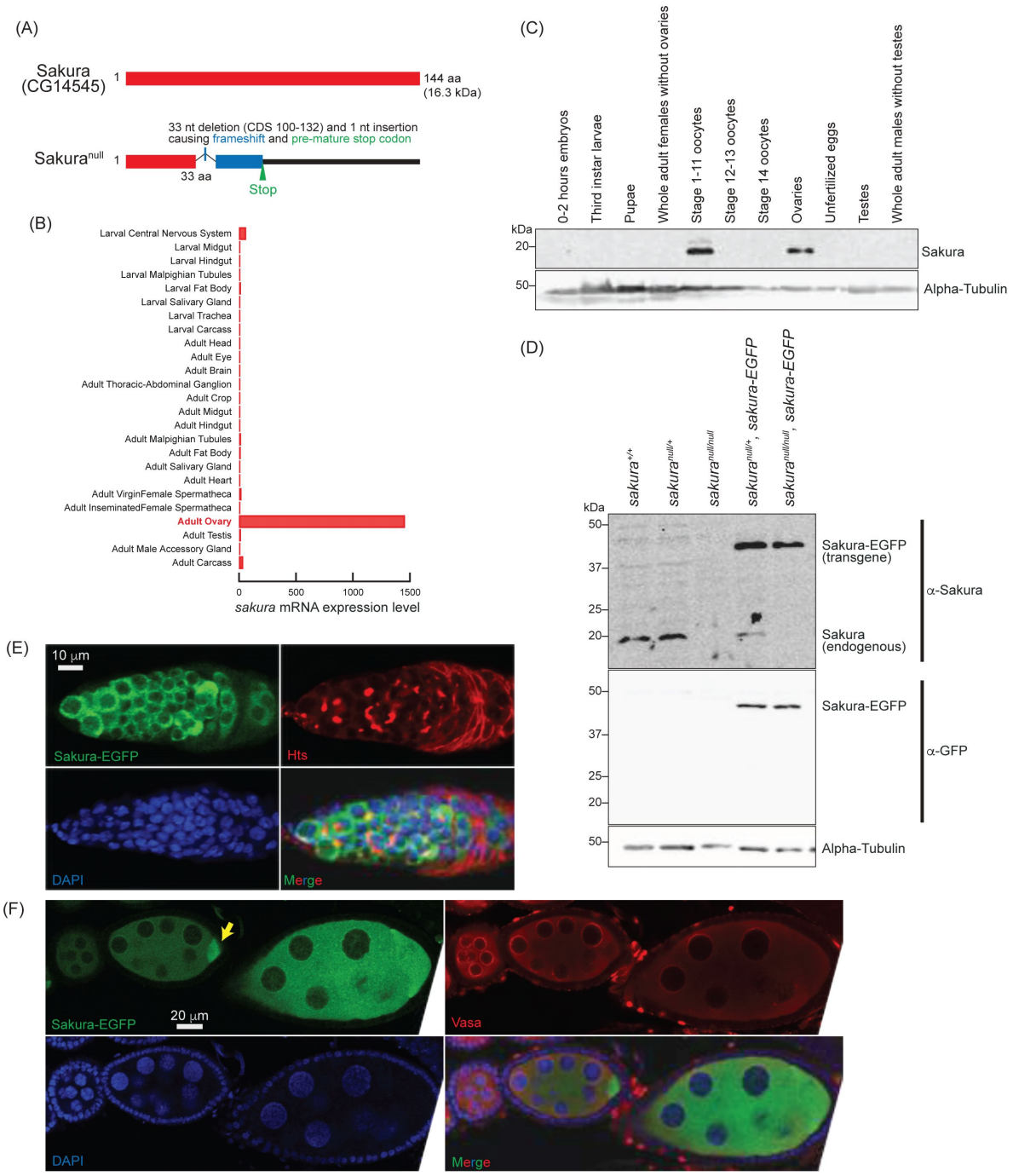

Fig 1.

Sakura expression pattern and mutant allele

(A) *Drosophila* Sakura protein (Sakura/CG14545) and its null mutant allele generated in this study. (B) *sakura* mRNA expression pattern. Data obtained from *http://flybase.org/reports/FBgn0040602.htm*. (C) Western blot of dissected fly tissues. (D) Western blot of ovary lysates. (E) Confocal images of the germarium from the *sakura-EGFP* transgenic fly. Sakura-EGFP (green), Hts (red), and DAPI (blue). Scale bar: 10 μm. (F) Confocal images of the egg chambers from the *sakura-EGFP* transgenic fly. Sakura-EGFP (green), Vasa (red), and DAPI (blue). Sakura-EGFP is expressed in nurse cells and enriched in the developing oocyte (yellow arrow). Scale bar: 20 μm.

sakura is essential for female fertility

Given its ovary-specific expression at both mRNA and protein levels (**Fig 1B** and **1C**), we hypothesized that Sakura plays a critical role in ovarian function. Fertility assays revealed that *sakura*$^{null/null}$ females laid no eggs when mated with wild-type males, while control female flies (*sakura*$^{+/+}$ and *sakura*$^{null/+}$) laid numerous eggs (**Fig 2A**). Dissection of *sakura*$^{null/null}$ ovaries revealed that they were rudimentary compared to normal ovaries in controls (**Fig 2C**). This suggests that the inability of *sakura*$^{null/null}$ female to lay eggs is due to their underdeveloped ovaries. In contrast, *sakura*$^{null/null}$ males were fertile and showed no significant differences compared to controls (*sakura*$^{+/+}$ and *sakura*$^{null/+}$) (**Fig S2**).

To confirm that the observed female sterility was caused by the loss of *sakura*, we generated *sakura* rescue flies expressing Sakura-EGFP in the *sakura*$^{null/null}$ background (*sakura*$^{null/null}$; *sakura-EGFP*). Western blotting confirmed that these flies expressed Sakura-EGFP, but not endogenous Sakura (**Fig 1D**). The *sakura-EGFP* transgene fully rescued both female fertility and ovary morphology in the *sakura*$^{null/null}$ background (**Fig 2**). *sakura-EGFP* rescue females showed no significant fertility differences compared to controls (**Fig 2A** and **2B**), and their ovaries were normal in shape and size (**Fig 2C**). We concluded that Sakura is essential for female fertility and normal ovary morphology but dispensable for male fertility, consistent with the observation that Sakura is predominantly expressed in ovarian germline cells (**Fig 1**).

sakura$^{null/null}$ ovaries are germless and tumorous

Given the rudimentary appearance of *sakura*$^{null/null}$ ovaries, we questioned whether they contained germ cells. We used flies carrying *vasa-EGFP* knocked-in reporter in the *sakura*$^{null/null}$ background, as Vasa is a known germ cell marker[7]. We observed that some *sakura*$^{null/null}$ ovarioles were devoid of germ cells ("germless"), while others retained germ cells (**Fig 3A**), suggesting that loss of *sakura* leads to germ cell depletion. Additionally, *sakura*$^{null/null}$ ovaries exhibited significantly higher levels of cleaved Caspase-3 staining, indicative of apoptosis, compared to controls (*sakura*$^{null/+}$) (**Fig 3B**).

Oogenesis begins in the germarium, which contains 2-3 GSCs identified by round, unbranched spectrosomes that contact cap cells[7] (**Fig S1**). In contrast, cysts have branched fusomes. Immunostaining with hu-li tai shao (HTS) antibody, which marks spectrosomes and fusomes, revealed an excess number of GSC-like cells with round spectrosomes in *sakura*$^{null/null}$ ovarioles containing germ cells (**Fig 3C**, red stars), indicative of a "tumorous" phenotype as previously described[27–29]. Additionally, we observed an excess number of cyst cells with branched fusomes that persisted throughout the ovarioles (**Fig 3C**), suggesting abnormal cyst cell differentiation and division.

Within the same ovary, some *sakura*$^{null/null}$ ovarioles exhibited the tumorous phenotype, while others were germless, without any spectrosome or fusome staining (**Fig 3C**, green stars). Quantification revealed that 35% of *sakura*$^{null/null}$ ovarioles were tumorous while the remaining 65% were germless (n=74) (**Fig 3D**). In contrast, no tumorous or germless phenotypes were observed in control (*sakura*$^{+/+}$ and *sakura*$^{null/+}$) or *sakura-EGFP* rescue flies (**Fig 3D**). Furthermore, ~95% of *sakura*$^{null/null}$ ovarioles with germ cells contained excess GSC-like cells (>5) (**Fig 3E** and **Fig S3**). The mean number of GSCs or GSC-like cells for *sakura*$^{+/+}$, *sakura*$^{null/+}$, and *sakura-EGFP* rescue was 2.2 ± 0.6, 2.2 ± 0.6, and 2.1 ± 0.7, respectively while that for *sakura*$^{null/null}$ was 26.5 ± 17.5 (p-value <0.05). These results suggest that Sakura is essential for regulating GSC division and differentiation. Overall, we conclude that Sakura is required for germ cell survival, division, and differentiation.

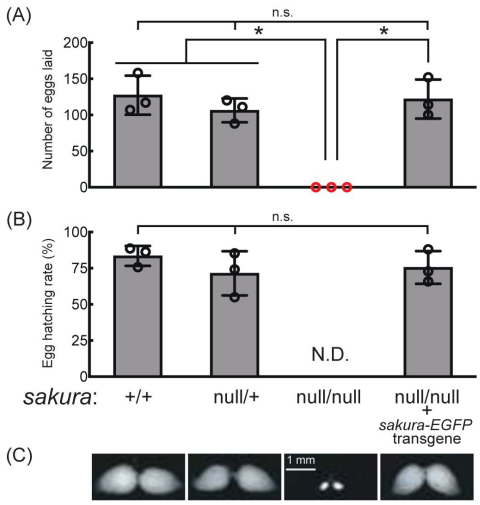

Fig 2.

sakura mutant flies are female-sterile and have rudimentary ovaries.

(A-B) Female fertility assays. (A) The number of eggs laid by test females crossed with OregonR wild-type males and (B) hatching rates of the eggs. Mean ± SD (n = 3). P-value < 0.05 (Student's t-test, unpaired, two-tailed) is indicated by *. (C) Stereomicroscope images of dissected whole ovaries. Scale bar: 1 mm.

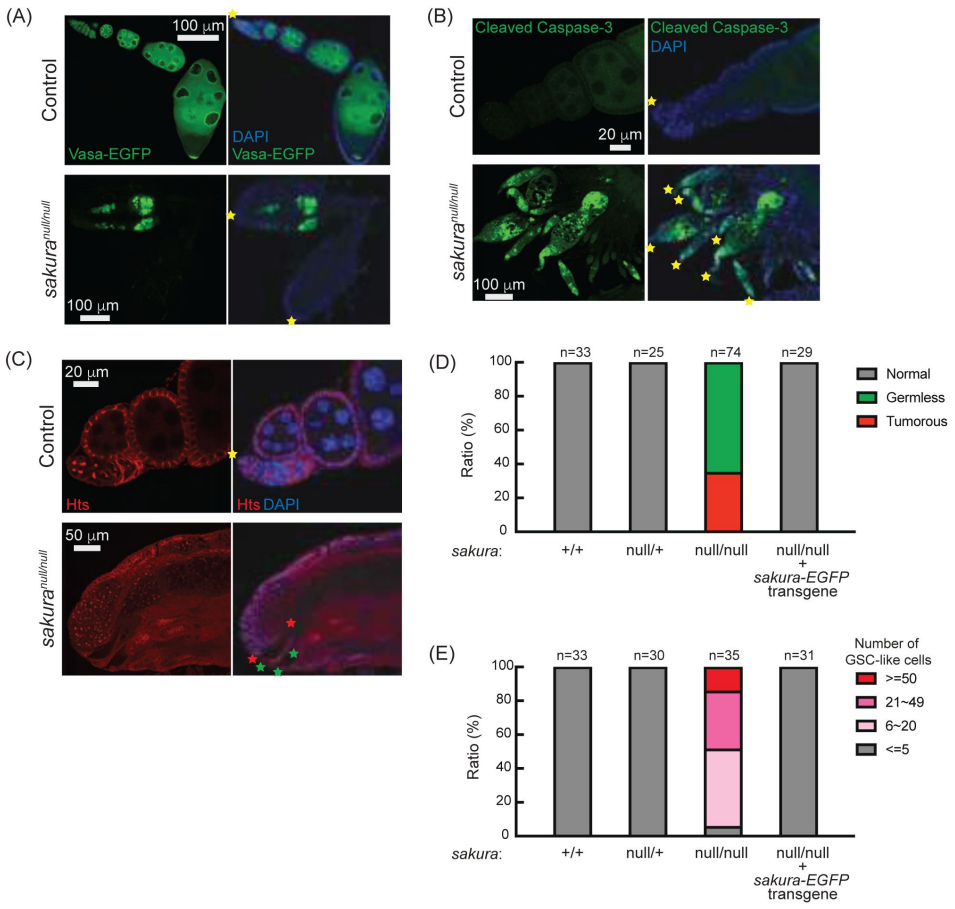

Fig 3.

sakura^{null} ovaries are germless and tumorous

(A) Confocal images of the ovaries from control (*sakura*$^{null/+}$) and *sakura*$^{null/null}$ harboring *vasa-EGFP*. Vasa-EGFP (green) and DAPI (blue). Yellow stars label the anterior tip of the ovaries. Scale bar: 100 μm. (B) Confocal images of *sakura*$^{null/null}$ ovaries stained with anti-cleaved Caspase-3 antibody. Cleaved caspase-3 (green) and DAPI (blue). Control ovary is *sakura*$^{null/+}$. Yellow stars label the anterior tip of the ovaries. Scale bars: 20 μm for control and 100 μm for *sakura*$^{null/null}$. (C) Confocal images of control (*sakura*$^{null/+}$) and *sakura*$^{null/null}$ ovaries stained with anti-Hts antibody to label spectrosomes and fusomes. Hts (red) and DAPI (blue). Yellow star labels the anterior tip in the control ovary. Red and green stars label the anterior tip of *sakura*$^{null/null}$ tumorous and germless ovarioles, respectively. Scale bars: 20 μm for control and 50 μm for *sakura*$^{null/null}$. (D) Ratio (%) of normal, germless, and tumorous ovaries of indicated genotypes (n=33, 25, 74, 29 respectively). (E) Quantification of GSC-like cell number in germaria of indicated genotypes (n = 33, 30, 35, and 31 respectively).

Loss of *sakura* results in reduced germline piRNA

Piwi-interacting RNAs (piRNAs) are produced in germline cells and somatic follicle cells and transcriptionally and post-transcriptionally silence transposon expression through sequence-complementarity. Disruption of the piRNA pathway can result in oogenesis arrest, germ cell loss, rudimentary ovaries, and sterility[9,30]. Loss of piRNAs in germ cells leads to the upregulation (desilencing) of transposons, increased DNA damage, and apoptotic cell death[31]. We investigated whether the loss of *sakura* would result in loss of piRNA and transposon upregulation. We performed high-throughput sequencing (small RNA-seq and polyA+ RNA-seq) on ovary RNA samples from $sakura^{+/+}$, $sakura^{null/+}$, $sakura^{null/null}$, and *sakura-EGFP* rescue ($sakura^{null/null}$ with *sakura-EGFP*) flies.

piRNA levels in $sakura^{null/null}$ ovaries were reduced compared to controls ($sakura^{+/+}$), while $sakura^{null/+}$ and *sakura-EGFP* rescue showed no such reduction (**Fig 4A**). Consistent with this, transposon RNA levels in $sakura^{null/null}$ ovaries were upregulated compared to $sakura^{+/+}$, while $sakura^{null/+}$ and *sakura-EGFP* rescue showed no such upregulation (**Fig 4B**). Given that Sakura is specifically expressed in germline cells, but not in somatic cells (**Fig 1E** and **1F**), we hypothesized that loss of *sakura* interrupts the piRNA pathway in germ cells, leading to the desilencing of germline transposons. A well-characterized germline transposon in *Drosophila* is *Burdock*[30,32]. We found that *Burdock* piRNA levels were significantly lower in $sakura^{null/null}$compared to controls and rescue flies (**Fig 4C**).

We employed the *Burdock* sensor, a transposon reporter tool to monitor germline piRNA activity[30]. The reporter expresses nuclear GFP and β-gal under the control of the *nanos* promoter for germline expression, with a target sequence for *Burdock* piRNAs in the 3' UTR[30] (**Fig 4D**). Using a *sakura* RNAi line driven by *UAS-Dcr2* and *NGT-Gal4* to knock down *sakura* specifically in the germline, we observed that GFP and β-gal expression were highly elevated in *sakura* knockdown germlines compared to control RNAi (y^{RNAi}) knockdowns (**Fig 4D**). This confirmed that loss of *sakura* leads to a loss of piRNA-mediated transposon silencing in the germline. We conclude that Sakura is essential for proper piRNA levels and piRNA-based transposon silencing in the germline.

sakura is important for oogenesis in germline cells beyond GSCs and germline cysts

Both $sakura^{null/null}$ and *sakura* germline RNAi knockdown driven by *UAS-Dcr-2* and *NGT-Gal4*, which initiates RNAi in germline from GSCs, resulted in rudimentary ovaries (**Fig 2C** and **5A**). These ovaries lacked later-stage germline cells and egg chambers, making it difficult to assess the role of Sakura beyond the germarium. However, because Sakura-EGFP expression is not limited to GSCs and germline cysts (**Fig 1E** and **1F**), we speculated that Sakura might function in later-stage germline cells as well.

To explore this possibility, we used *TOsk-Gal4* (a combination of *osk-Gal4* and *αTub67C-Gal4*) to drive *sakura* RNAi knockdown in germline cells after the germline cyst stage (from germarium region 2b onward. **Fig S1A**), sparing GSCs and germline cysts[33]. Unlike *NGT-Gal4*, *TOsk-Gal4*-driven *sakura* RNAi knockdown did not drastically affect ovary morphology (**Fig 5A**), allowing us to study the effects of *sakura* loss in egg chambers. We confirmed *sakura* RNAi (*sakura RNAi #1* and #2) knockdown efficiency by Western blot, showing effective depletion of Sakura in ovaries from both *NGT-Gal4* and *TOsk-Gal4*-driven RNAi lines (**Fig 5B**).

Interestingly, *TOsk-Gal4*-driven *sakura* RNAi knockdown severely reduced the numbers of eggs laid (**Fig 5C**) and stage 14 oocytes in ovaries compared to control RNAi (y^{RNAi}) (**Fig 5D**), suggesting that *sakura* is important for oogenesis beyond the germline cyst stage. Additionally, we observed mislocalized and dispersed Oo18 RNA-binding protein (Orb. A marker for oocyte

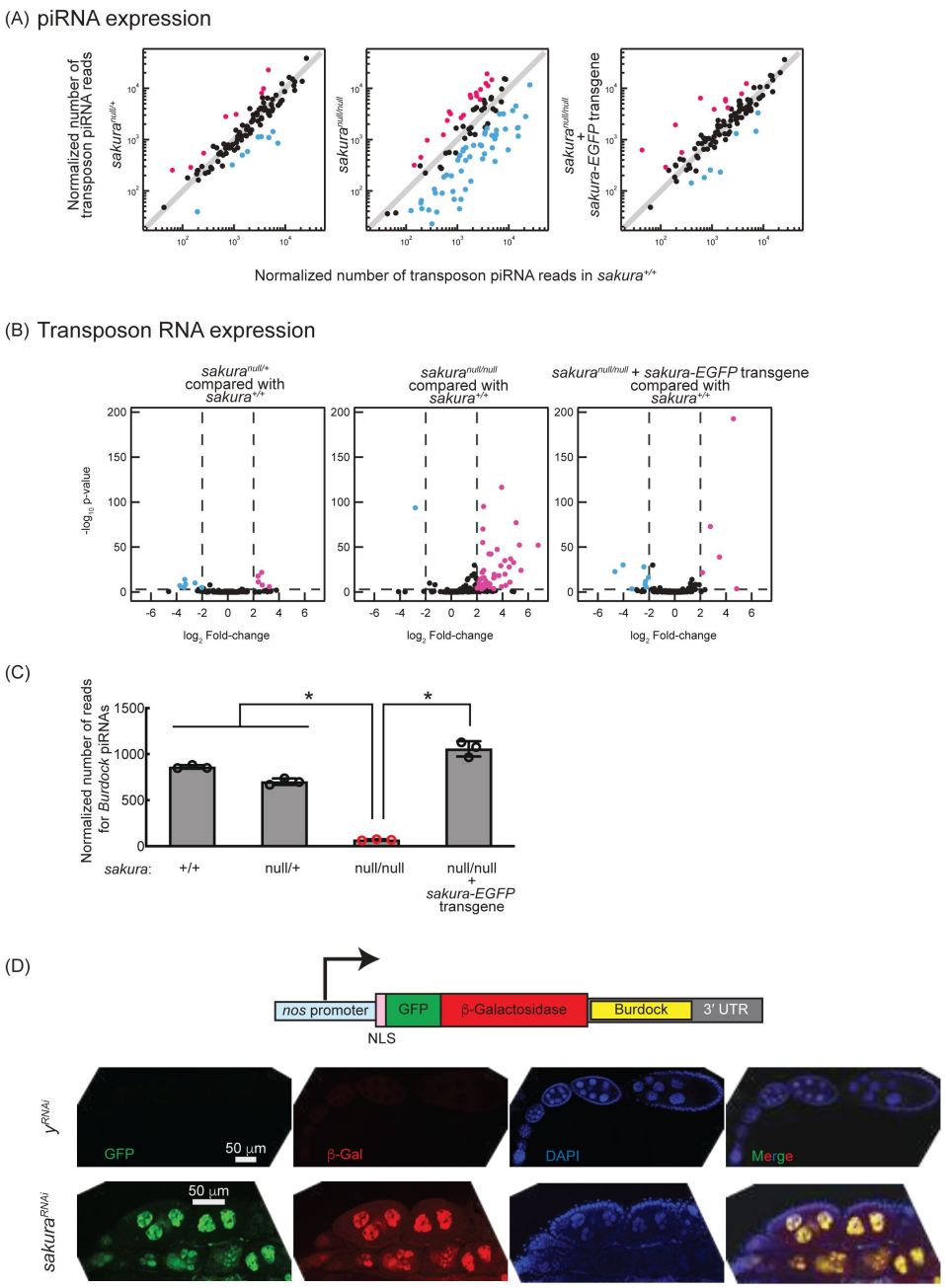

Fig 4.

Loss of *sakura* results in lower piRNA levels and loss of piRNA-mediated transposon silencing

(A) Scatter plots of normalized number of transposon piRNA reads from small RNA-seq of indicated genotypes compared with *sakura*$^{+/+}$. Means of three biological replicates are plotted. Downregulated (fold-change < 0.5) and upregulated (fold-change > 2) transposon piRNAs are shown in cyan and magenta, respectively. (B) Volcano plots of transposon RNAs from RNA-seq of indicated genotypes compared with *sakura*$^{+/+}$. Three biological replicates per genotype were analyzed. Downregulated (adjusted p-value < 0.001 and $\log_2$(fold-change) < -2) and upregulated (adjusted p-value < 0.001 and $\log_2$(fold-change) > 2) transposons are shown in cyan and magenta, respectively. (C) Normalized number of reads for *Burdock* piRNAs from small RNA-seq. Mean ± SD (n = 3.) P-value < 0.05 (Student's t-test, unpaired, two-tailed) is indicated by *. (D) The *Burdock* sensor harbors a *nanos* promoter, a nuclear localization signal (NLS) appended to GFP and β-gal coding sequences, and a target sequence for *Burdock* piRNAs in the 3'UTR. Confocal images of ovaries from control (y^{RNAi}) and *sakura*^{RNAi} flies harboring the Burdock sensor, where RNAi knockdown was specifically driven in the female germline with *UAS-Dcr2* and *NGT-Gal4*. GFP (green), β-gal (red), and DAPI (blue). Scale bar: 50 μm.

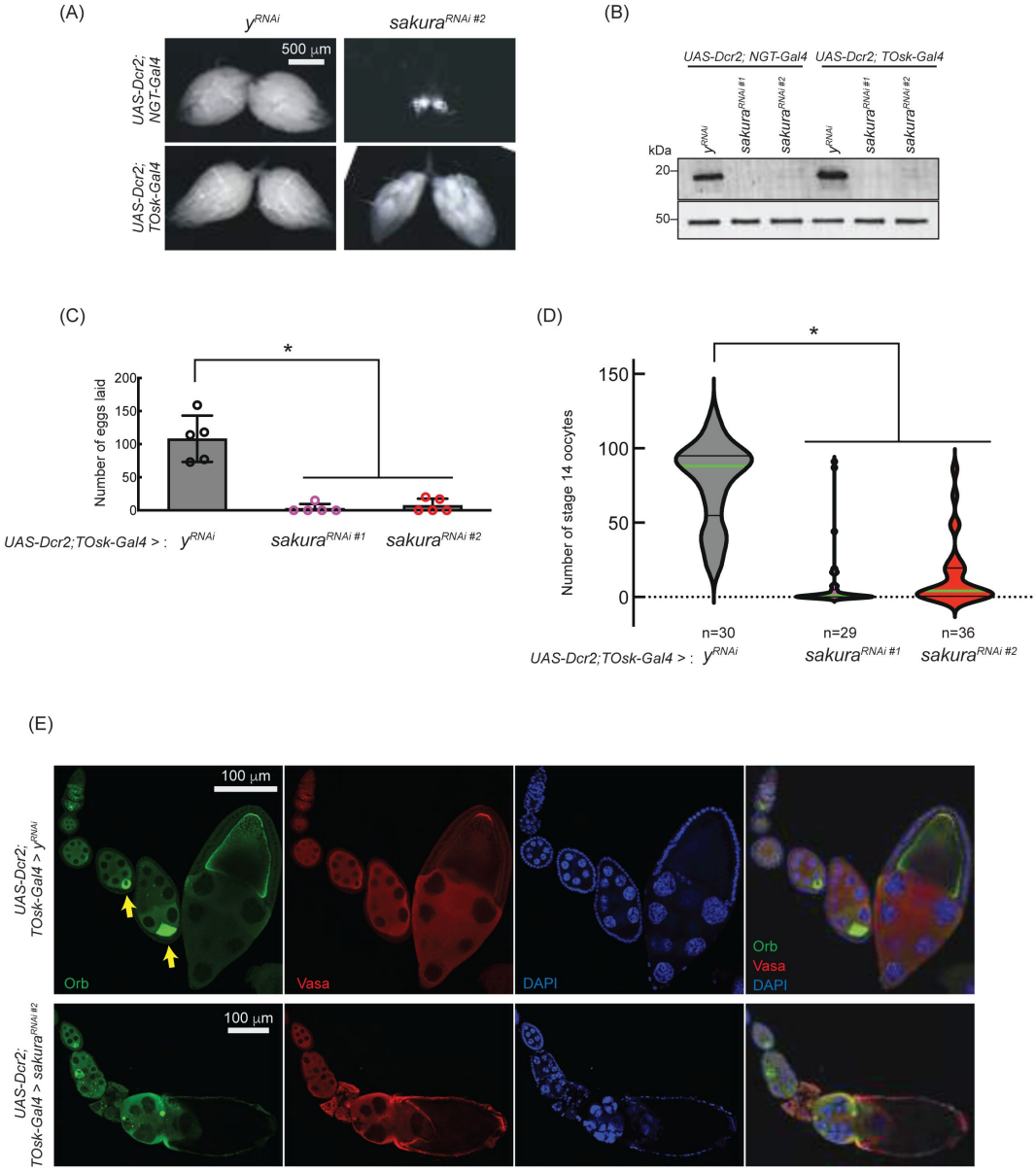

Fig 5.

sakura is important for oogenesis in later-stage egg chambers

(A) Stereomicroscope images of dissected whole ovaries. Scale bar: 500 μm. (B) Western blot of dissected ovary lysates. *sakura*$^{RNAi\ \#1}$ and *sakura*$^{RNAi\ \#2}$ are two independent RNAi lines. (C) Number of eggs laid by *sakura* RNAi knockdown driven by *UAS-Dcr2* and *TOsk-Gal4*. Mean ± SD (n = 5). P-value < 0.05 (Student's t-test, unpaired, two-tailed) is indicated by *. (D) Number of stage 14 oocytes produced by *sakura* RNAi knockdown flies driven by *UAS-Dcr2* and *TOsk-Gal4*. P-value < 0.05 (Student's t-test, unpaired, two-tailed) is indicated by *. (E) Confocal images of the ovaries from *sakura* RNAi knockdown flies driven by *UAS-Dcr2* and *TOsk-Gal4*, stained with anti-Orb and anti-Vasa antibodies. Orb (green), Vasa (red), and DAPI (blue). Yellow arrows label the localization and enrichment of Orb in the developing oocytes. Scale bar: 100 μm. In A-E, *y-RNAi* was used as a control.

identity) in *TOsk-Gal4*-driven *sakura* RNAi knockdowns (**Fig 5E**). Proper Orb localization is critical for oocyte specification and maintenance[34], and its mislocalization likely underlies the reduced ability to produce stage 14 oocytes and eggs *sakura* knockdown flies (**Fig 5C** and **5D**). We conclude that Sakura is crucial for proper Orb localization and in germline cells beyond GSCs and germline cysts. In subsequent *sakura* RNAi experiments, we used the *sakura RNAi* #2 line.

Sakura is required intrinsically for GSC establishment, maintenance, and differentiation

To explore whether *sakura* functions autonomously in the germline, we conducted mosaic analysis using the FLP-FRT system[35]. First, we assessed its role in GSC establishment by marking $sakura^{null}$ clones in primordial germ cells (PGCs)) before the early third instar larval stage and tracking their development into adult GSCs, as described in a previous study[36]. In control adult flies,12.3% (20/163) of GSCs were marked, while only 1.9% (4/213) were marked in $sakura^{null}$mutants, demonstrating that *sakura* is autonomously important for GSC establishment.

Next, we assessed GSC maintenance by generating marked $sakura^{null}$GSCs in adult flies using the FLP-FRT system and measuring their loss rate over time [14,36]. The percentage of marked control GSC clones and marked $sakura^{null}$ GSC clones 4 days after clone induction was 27.8% and 22.1%, respectively (**Fig 6A**). These numbers were considered the initial percentage. The percentage of marked control GSCs decreased to 25.8% and 16.8% on days 7 and 14, respectively (**Fig 6A**), resulting in a loss rate of 39.4% over the 10-day testing period (from day 4 to day 14). In contrast, the percentage of marked $sakura^{null}$ GSC clones decreased to 16.3% and 5.4% on days 7 and 14, respectively. Thus, the loss rate of $sakura^{null}$ GSCs is 75.6% over the 10-day period, which is higher than controls. We conclude that *sakura* is intrinsically required for GSC maintenance.

Germline depletion of *sakura* caused germless and tumorous phenotypes (**Fig 3**). To determine whether *sakura* is intrinsically required in the germ line cells for GSC differentiation, we quantified the number of marked (GFP-negative) and unmarked (GFP-positive) GSC-like cells (germline cells with a round spectrosome) in the germaria carrying marked GSC clones at 4, 7, and 14 days after clone induction. We found that the number of marked $sakura^{null}$GSC-like cells was higher than that of marked control GSC-like cells at all time points (**Fig 6C**). The number of marked $sakura^{null}$GSC-like cells increased over the 10-day period, while the number of marked control cells did not (**Fig 6C**). In contrast, the number of unmarked GSC-like cells in germaria containing $sakura^{null}$ GSC clones did not differ significantly from those in germaria containing control GSC clones, and the number did not increase (**Fig S4**). These results indicate that *sakura* is intrinsically important in germline cells, including GSCs, to regulate their proper division and differentiation. Taken together, we conclude that *sakura* is required intrinsically for GSC establishment, maintenance, and differentiation.

Loss of *sakura* inhibits Dpp/BMP signaling

Dpp/BMP signaling is a key pathway regulating GSC self-renewal and differentiation (**Fig S1**)[7,37]. We hypothesized that the germless and tumorous phenotypes observed in *sakura* loss-of-function ovaries could be due to Dpp/BMP signaling misregulation. To test this, we knocked down *sakura* in the germline driven by *UAS-Dcr2* and *NGT-Gal4* in the presence of *bam-GFP* reporter[38]. In controls (y^{RNAi}), Bam-GFP expression was restricted to 8-cell cysts and disappeared in 16-cell cysts and onward (**Fig 7A**)[38]. However, in *sakura* knockdowns, Bam-GFP expression persisted throughout the ovariole, with excess Bam-GFP positive cells (**Fig 7A**). This suggests that Bam expression is not repressed by Dpp/BMP signaling, leading to GSC loss in *sakura* knockdowns.

To further confirm this finding, we used the FLP-FRT technique to induce $sakura^{null}$ clones in the germaria and stained them with anti-Bam antibody[20]. All $sakura^{null}$ clones expressed Bam throughout the germarium, whereas in control clones, Bam was not expressed in the GSCs and

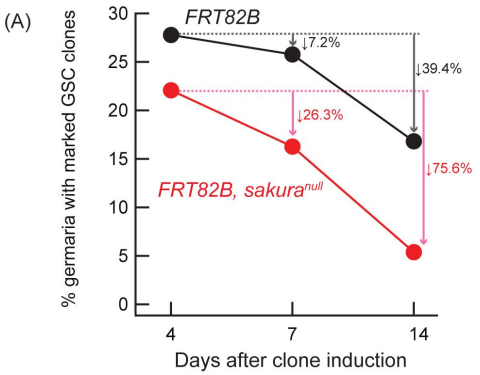

Genotype	Days after stopping heat shock	% marked GSCs	Relative % marked GSCs	Total number of germaria examined
hs-flp; +; *FRT82B, ubi-GFP* / *FRT82B* (control)	4	27.8	100	108
	7	25.8	92.8	97
	14	16.8	60.6	101
hs-flp; +; *FRT82B, ubi-GFP* / *FRT82B, sakura^null*	4	22.1	100	77
	7	16.3	73.7	86
	14	5.4	24.4	167

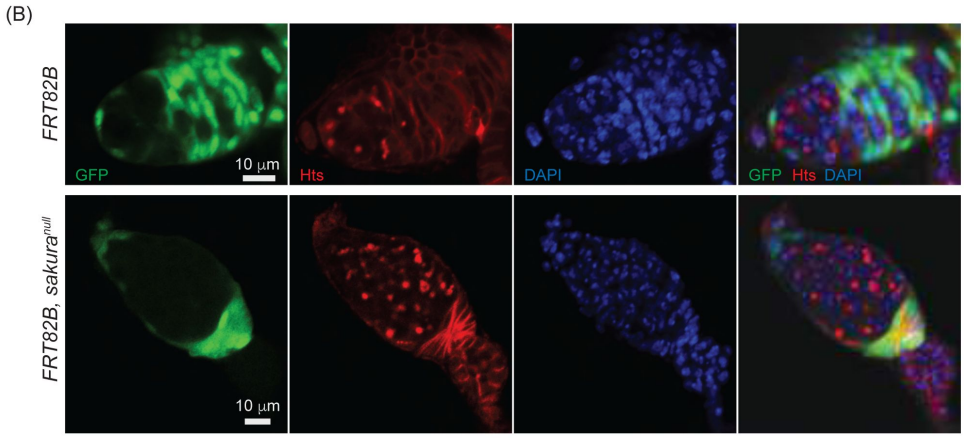

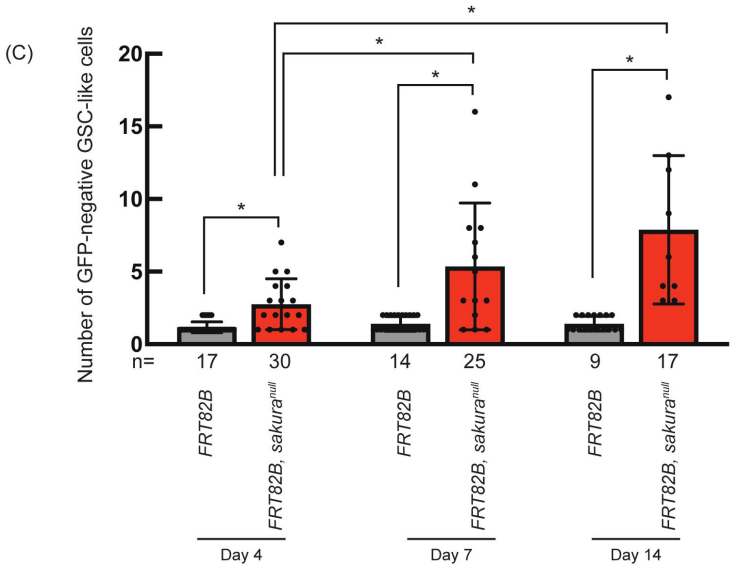

Fig 6.

Germline clonal analysis of *sakura^null*

(A) Percentage of germaria with marked GSC clones indicated by the absence of GFP at 4, 7, and 14 days after clone induction at the adult stage. Arrows indicate the percent decrease of marked GSC clones compared to day 4. The genotype, actual percentage, and total number of germaria examined are shown in the adjacent table. (B) Confocal images of germ cell clones. *sakura^null* and control clones were marked by the absence of GFP. GFP (green), Hts (red), and DAPI (blue). Scale bar: 20 μm. (C) Number of marked (GFP-negative) GSC-like cells in germaria with marked GSCs of the indicated genotypes at 4, 7, and 14 days after clone induction. GSC-like cells containing round spectrosome were identified through immunostaining with anti-Hts antibody. P-value < 0.05 (Student's t-test, unpaired, two-tailed) is indicated by *.

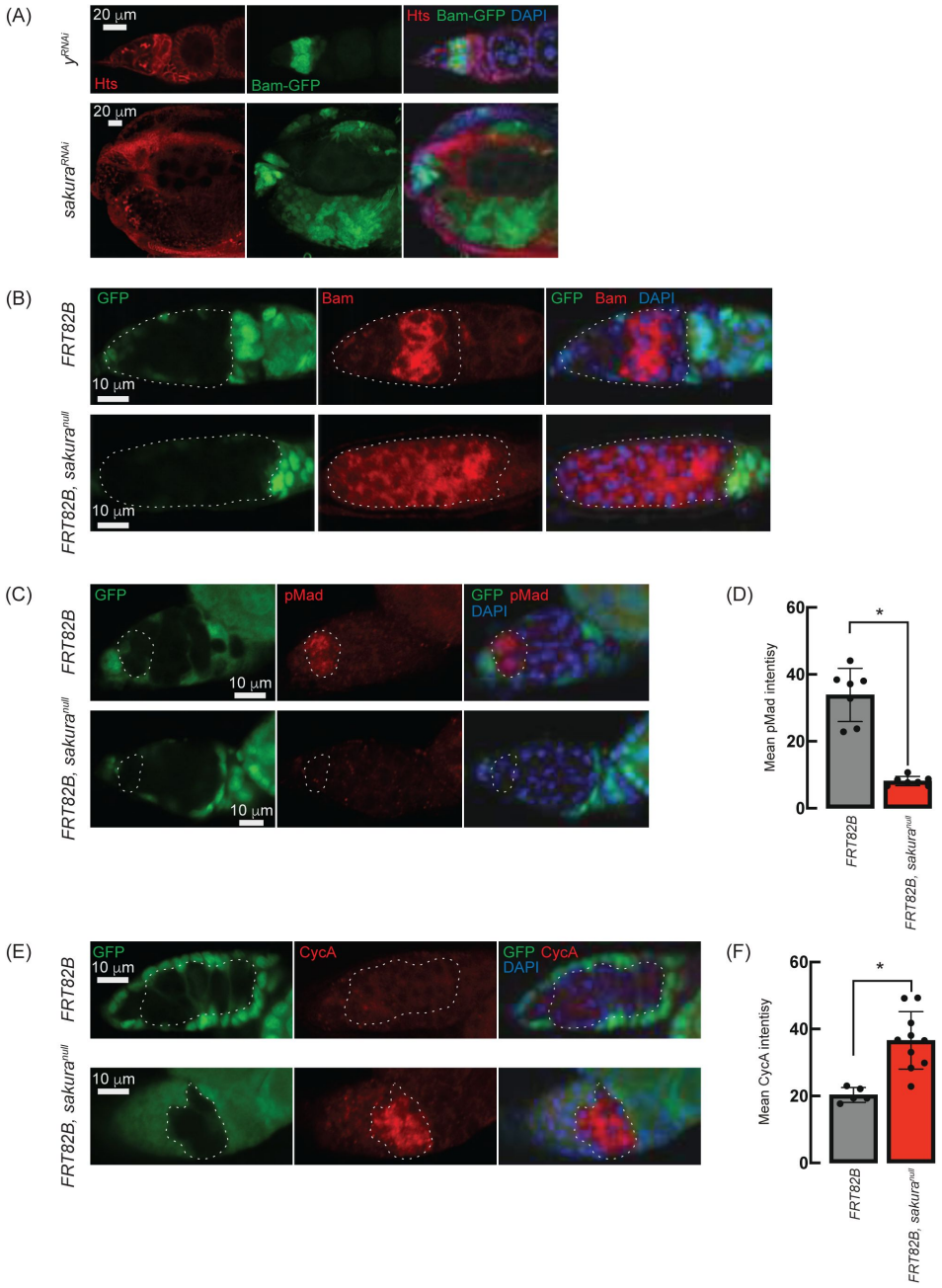

Fig 7.

Loss of *sakura* inhibits Dpp/BMP signaling

(A) Confocal images of ovaries from control (y^{RNAi}) and $sakura^{RNAi}$ flies harboring the *bam-GFP* reporter, where RNAi knockdown was specifically driven in the female germline with *UAS-Dcr2* and *NGT-Gal4*. Bam-GFP (green), Hts (red), and DAPI (blue). Scale bar: 20 μm. (B, C) Confocal images of germaria with germline clones of $sakura^{null}$ stained with (B) anti-Bam antibody and (C) anti-pMad antibody. GFP (green), Bam or pMad (red), and DAPI (blue). Scale bar: 10 μm. (D) Mean pMad intensity in the germline clones of the indicated genotypes. Mean ± SD (n = 7). P-value < 0.05 (Student's t-test, unpaired, two-tailed) is indicated by * (E) Confocal images of germaria with germline clones of $sakura^{null}$ stained with anti-CycA antibody. GFP (green), CycA (red), and DAPI (blue). Scale bar: 10 μm. (F) Mean CycA intensity in the germline clones of the indicated genotypes. Mean ± SD (n = 5 and 10 for *FRT82B* and *FRT82B, sakura*^{null} respectively). P-value < 0.05 (Student's t-test, unpaired, two-tailed) is indicated by *. In B, C, and E, clones were marked with the absence of GFP.

was restricted to cyst cells (**Fig 7B**). In GSCs, pMad translocates into the nucleus to repress Bam expression [16,17] (**Fig S1**). We stained ovaries with anti-pMad antibodies and found that pMad intensity was significantly reduced in *sakura*^{null} GSC clones compared to control GSCs (**Fig 7C** and **D**). This indicates that the dysregulated Bam expression observed in *sakura*^{null} was due to reduced pMad levels in GSCs.

Previous studies have shown that ectopic expression of a stable form of CyA leads to germ cell loss [39]. This germ cell loss phenotype is also observed upon ectopic *bam* expression in GSCs [14,40,41]. It was reported that Bam associates with Ovarian tumor (Otu) to promote deubiquitination and stabilization of CycA [21]. Since we observed derepressed *bam* expression in *sakura*^{null} cells, we investigated whether CycA levels were affected. Staining ovaries with anti-CycA antibodies revealed higher CycA intensity in *sakura*^{null} clones compared to neighboring wild-type cells in the same germarium and control clones in control germarium (**Fig 7E**). *sakura*^{null} clones exhibited significantly higher mean CycA intensity compared to control clones (**Fig 7F**). The elevated CycA levels in *sakura*^{null} clones likely results from Bam misexpression and Bam-mediated stabilization.

Finally, we tested whether we could rescue the germless phenotype caused by *sakura* loss-of-function by knocking down either *bam* or *cycA* in the germline. Double RNAi knockdown of *sakura* and *bam* in the germline using *UAS-Dcr-2* and *NGT-Gal4* partially rescued the germless phenotype (**Fig 8**). In contrast, knocking down *sakura* and *cycA* together failed to rescue the germless phenotype (**Fig 8**). This suggests that the germless phenotype of *sakura* is partly due to *bam* misexpression, not *cycA*.

Sakura binds Otu

To explore the molecular function of Sakura in oogenesis, we aimed to identify Sakura-interacting proteins. We conducted a co-immunoprecipitation experiment using anti-GFP magnetic beads on the ovary lysates of flies expressing Sakura-EGFP, followed by mass spectrometry to identify co-immunoprecipitated proteins. Ovary lysates from flies without the *sakura-EGFP* transgene (*w1118*) served as negative controls. Mass spectrometric analysis revealed several proteins with peptide signals present in all three biological replicates of the Sakura-EGFP samples without any signals in any of the three biological replicates of the negative control (**Table 1**). Among these, the most promising candidate, exhibiting the highest unique peptide signal in each of three replicates of the Sakura-EGFP samples was Otu.

To confirm this finding, we generated a polyclonal anti-Otu antibody. Using Western blot analysis, we detected endogenous Otu protein in the Sakura-EGFP immunoprecipitants from ovaries, but not in the negative control (**Fig 9A**), validating the mass spectrometry results. Next, using wild-type (without Sakura-EGFP) ovary lysates, we immunoprecipitated endogenous Sakura with anti-Sakura antibody and detected endogenous Otu in the immunoprecipitant by Western blot (**Fig 9B**), demonstrating that endogenous Sakura interacts with endogenous Otu. Furthermore, we found that ectopically expressed Flag-tagged Otu co-immunoprecipitated with ectopically expressed HA-tagged Sakura in S2 cells (**Fig 9C**).

The *otu* gene encodes two annotated protein isoforms, a predominant 98 kDa isoform and a less abundant 104 kDa isoform resulting from alternative splicing [42]. The 98kDa isoform lacks Tudor domain encoded in an alternatively spliced 126-bp exon [43]. It has been reported that the 104 kDa Otu isoform can perform all functions, while the 98 kDa Otu isoform functions in later stages of oogenesis, such as nurse cell regression and oocyte maturation [44]. The major Otu isoform observed in the inputs and immunoprecipitates from ovaries in **Figure 9** corresponds to the 98 kDa isoform.

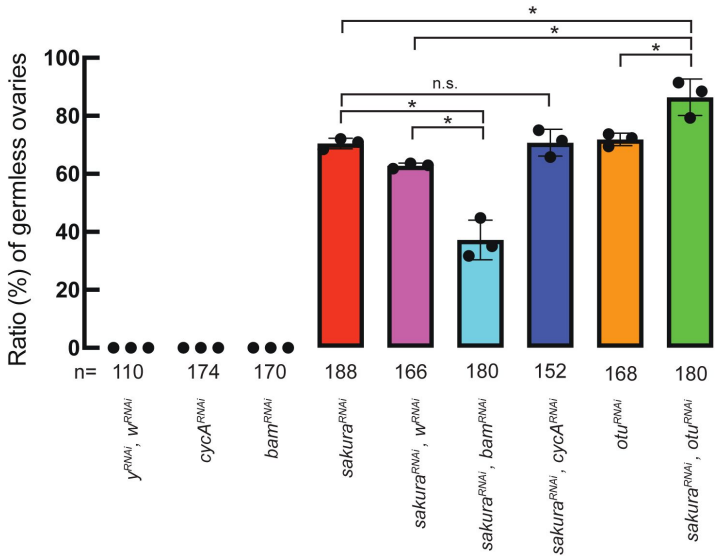

Fig 8.

The ratio of ovary germless phenotype from double RNAi knockdown of *sakura* with *bam*, *cycA*, or *otu*

Mean ratio (%) of ovaries with the germless phenotype observed in double RNAi knockdown of *sakura* with *bam, cycA,* or *otu. UAS-Dcr2* and *NGT-Gal4* was used to drive RNAi knockdown in the germline. n is the total number of ovaries examined for the indicated genotypes. Three independent crosses (biological replicates) were set up to generate the flies with genotypes of interest, and the ratio of ovaries with the germless phenotype in each replicate was calculated. Mean ± SD (three biological replicates). P-value < 0.05 (Student's t-test, unpaired, two-tailed) is indicated by *.

Table 1.

Number of unique peptide counts detected by mass-spec.

Proteins with peptide signals present in all three biological replicates of the Sakura-EGFP samples without any signals in any of the three biological replicates of the negative control are shown.

Identified protein name	Gene ID	Unique peptide counts					
		Sakura-EGFP samples			w1118 samples (negative control)		
		Replicate 1	Replicate 2	Replicate 3	Replicate 1	Replicate 2	Replicate 3
Ovarian tumor	CG12743	44	38	18	0	0	0
Uncharacterized protein Dmel_CG4679	CG4679	17	8	2	0	0	0
Uncharacterized protein Dmel_CG14997	CG14997	17	7	2	0	0	0
Mitochondrial ribosomal protein S22	CG12261	14	6	1	0	0	0
Tudor	CG9450	15	1	1	0	0	0
Mitochondrial ribosomal protein S5	CG40049	10	4	1	0	0	0
HECT and RLD domain containing protein 2	CG11734	4	9	1	0	0	0
Mitochondrial ribosomal protein S10	CG4247	5	3	1	0	0	0
Mitochondrial ribosomal protein S31	CG5904	3	1	1	0	0	0
Uncharacterized protein Dmel_CG1316	CG1316	2	1	1	0	0	0

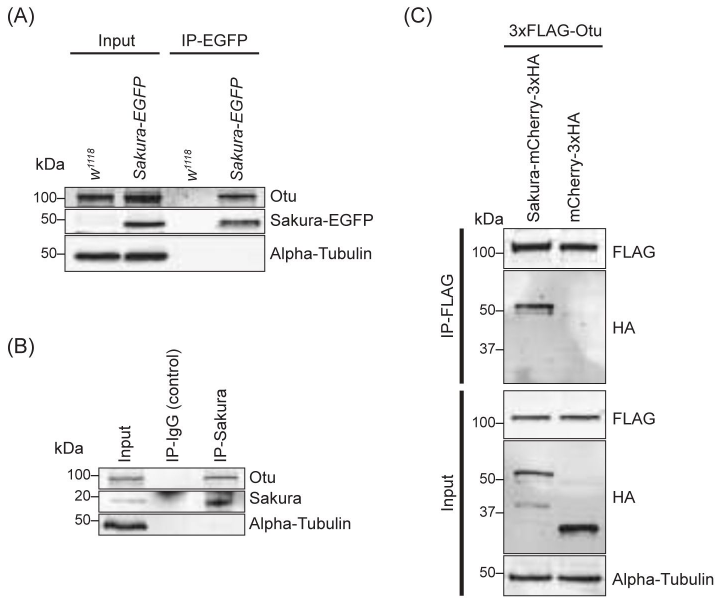

Fig 9.

Sakura interacts with Otu.

(A) Co-immunoprecipitation using anti-GFP magnetic beads followed by Western blotting. Ovary lysates expressing Sakura-EGFP and those from w^{1118}negative control were tested. (B) Co-immunoprecipitation using beads bound with rabbit anti-Sakura followed by Western blotting. Ovary lysates from w^{1118} flies were used. Rabbit IgG was used as control IP. (C) Co-immunoprecipitation using beads bound with anti-FLAG antibody followed by Western blotting. S2 cell lysates expressing 3xFLAG-Otu and Sakura-mCherry-3xHA or mCherry-3xHA (negative control) were used.

Next, we sought to identify which regions of Sakura and Otu are important for their interaction. We predicted the structure of the Sakura-Otu protein complex using AlphaFold[45]. AlphaFold suggests that the N-terminal region of Sakura (1-49aa) and the N-terminal region of Otu (1-405aa) are highly likely to form interactions, while the C-terminal region of Sakura (100-144aa) does not interact with Otu (**Fig 10A-C**). The Tudor domain of Otu is not directly involved in this interaction. To experimentally validate the predictions made by AlphaFold, we generated a series of truncated Otu fragments, including Otu(ΔTudor) (1-336, 389-853aa, corresponding to the endogenous 98 kDa isoform), Otu(N1) (1-405aa), Otu(N2) (1-339aa), and Otu(C) (405-853aa) (**Fig 10B**). We then performed co-immunoprecipitation assays to test which fragments could interact with full-length Sakura. All fragments except Otu(C) were associated with full-length Sakura protein in S2 cells (**Fig 10D**), demonstrating that the C-terminal low-complexity region of Otu is dispensable for the interaction. This assay also showed that the Tudor domain is not critical and the N-terminal fragment (1-339aa) of Otu is sufficient for interaction with Sakura. These findings align well with the predictions made by AlphaFold.

Subsequently, we created several truncated Sakura fragments and conducted co-immunoprecipitation assays in S2 cells to determine which Sakura fragments can interact with full-length Otu. The fragments generated included Sakura(NM) (1-100aa), Sakura(NC) (1-49, 100-144aa), Sakura(MC) (49-144aa), Sakura(N) (1-49aa), Sakura(M) (49-100aa), and Sakura(C) (100-144aa) (**Fig 10C**). We found that Sakura(NM), Sakura(NC), Sakura(N), and Sakura(M) were associated with Otu (**Fig 10E**). Compared to Sakura(NM) and Sakura(N), the interaction of Sakura(M) with Otu is relatively weaker, as indicated by a fainter band in the Western blot (**Fig 10E**). Sakura-NC exhibited a weak interaction with Otu, while Sakura(MC) and Sakura(C) showed no interaction (**Fig 10E**). These assays demonstrated that the N-terminal region (1-49aa) of Sakura is sufficient for interaction with Otu. Moreover, the results suggest that the C-terminal region of Sakura (100-144aa) does not interact with Otu and that adjoining it with the N-terminal (1-49aa) or the middle (M) region (49-100aa) weakens the interaction with Otu. These findings support the AlphaFold predictions.

Finally, to test whether the interaction between Sakura and Otu can be achieved solely through their N-terminal regions, we performed co-immunoprecipitation assay with Sakura(N) and Otu(N2). We discovered that they interact each other (**Fig 10F**). A reciprocal co-immunoprecipitation assay also confirmed their interaction (**Fig S5**), revealing that the interaction between Sakura and Otu can be established with just the 1-49aa of Sakura and the 1-339aa of Otu. Therefore, we conclude that Sakura interacts with Otu *in vivo,* and the N-terminal regions of both proteins are sufficient for their interaction.

Loss of *otu* phenocopies loss of *sakura*

Having established the interaction between Sakura and Otu, we were interested in whether they function together during oogenesis. We speculated that for them to interact and function together, Sakura and Otu must exhibit similar expression and localization patterns in ovaries. We generated two transgenic flies carrying full-length *otu-EGFP* or *otu(ΔTudor)-EGFP* transgenes; both constructs are C-terminally fused with EGFP and under the control of the *otu* promoter. We found that both Otu-EGFP and Otu(ΔTudor)-EGFP display similar expression and localization patterns to Sakura-EGFP (**Fig 1E**, 1F and **Fig 11A**). Like Sakura-EGFP, Otu-EGFP and Otu(ΔTudor)-EGFP are specifically expressed in germ cells, but not in follicle cells, and are localized to the cytoplasm, being enriched in the developing oocytes (**Fig 11A**). We did not observe any difference in localization patterns between Otu-EGFP and Otu(ΔTudor)-EGFP; suggesting that the Tudor domain is not crucial for Otu protein localization. Notably, the localization pattern exhibited by the transgenic Otu-EGFP generated in this study is consistent with a previous report [23].

Previous studies have shown that mutations in *otu* lead to severe defects in germ cell division and differentiation, resulting in a tumorous phenotype[22–24,42]. To study the role of *otu* specifically in the germline, we performed RNAi knockdown of *otu* in the germline driven by *nos-*

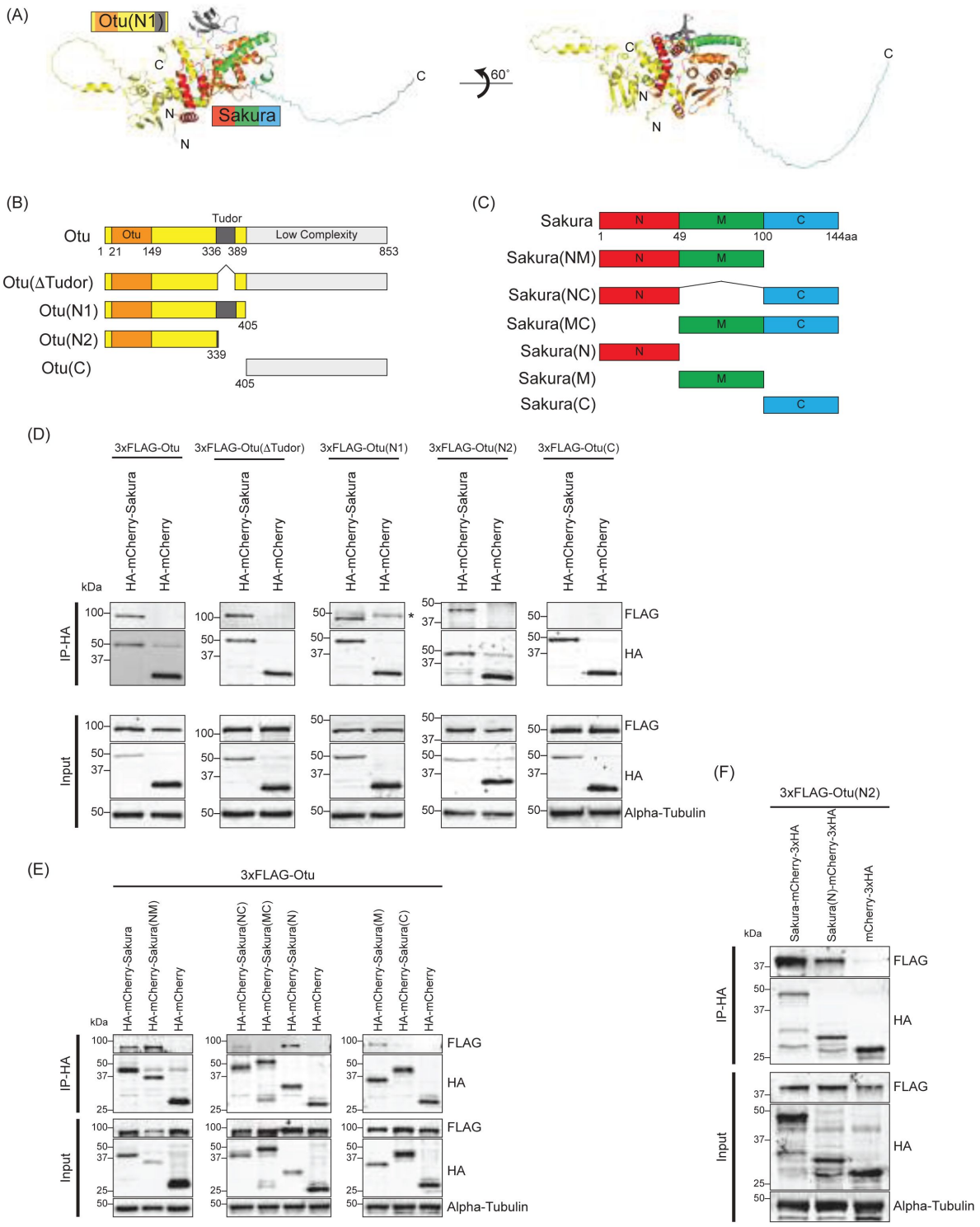

Fig 10.

N-terminal regions of Sakura and Otu are important for interaction.

(A) Predicted structure of the Sakura and Otu protein complex made by AlphaFold. Full-length Sakura and N-terminal Otu fragment (N1. 1-405aa) were used for prediction. (B) Full-length Otu and Otu fragments tested in co-immunoprecipitation assays. (C) Full-length Sakura and Sakura fragments tested in co-immunoprecipitation assays (N: N-terminal, M: middle, C: C-terminal). (D, E, F) Co-immunoprecipitation using anti-HA magnetic beads followed by Western blotting. S2 cell lysates expressing HA-tagged mCherry were used as negative controls.

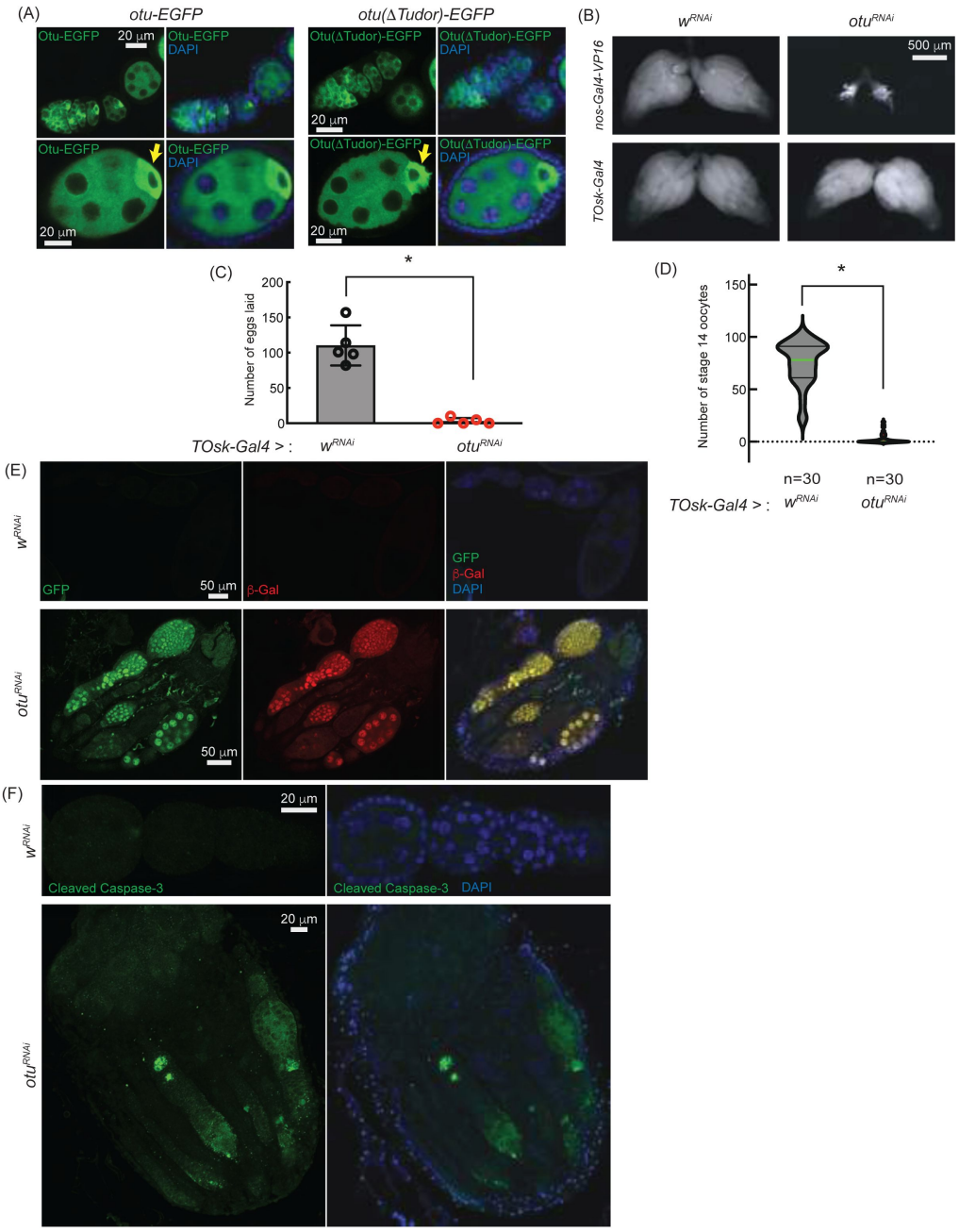

Fig 11.

Loss of *otu* phenocopies loss of *sakura*

(A) Confocal images of ovaries from *otu-EGFP* and *otu(ΔTudor)-EGFP* transgenic flies. Otu-EGFP and Otu(ΔTudor)-EGFP (green), DAPI (blue). Yellow arrows show the enrichment of Otu-EGFP and Otu(ΔTudor)-EGFP in developing oocytes. Scale bar: 20 μm. (B) Stereomicroscope images of dissected whole ovaries from w^{RNAi} (control) and otu^{RNAi} flies where RNAi knockdown was driven in the female germline with *nos-Gal4-VP16* or *TOsk-Gal4*. Scale bar: 500 μm. (C) Number of eggs laid by *TOsk-Gal4* > w^{RNAi} and *TOsk-Gal4* > otu^{RNAi} flies. Mean ± SD (n = 5). P-value < 0.05 (Student's t-test, unpaired, two-tailed) are indicated by *. (D) Violin plots of the number of stage 14 oocytes produced in *TOsk-Gal4* > w^{RNAi} and *TOsk-Gal4* > otu^{RNAi} flies. n = 30. P-value < 0.05 (Student's t-test, unpaired, two-tailed) is indicated by *. (E) Confocal images of the ovaries from w^{RNAi} (control) and otu^{RNAi}flies harboring the Burdock sensor where RNAi knockdown was driven in the female germline with *UAS-Dcr2* and *NGT-Gal4*. GFP (green), β-gal (red), and DAPI (blue). Scale bar: 50 μm. (F) Confocal images of the ovaries from *nos-Gal4-VP16* > w^{RNAi} and *nos-Gal4-VP16* > otu^{RNAi} flies stained with anti-cleaved Caspase 3 antibody. Cleaved Caspase-3 (green) and DAPI (blue). Scale bar: 20 μm

Gal4-VP16. Interestingly, we found that germline depletion of *otu* results in rudimentary ovaries, similar to the loss of *sakura* (**Fig 2D**, **Fig 5A**, and **Fig 11B**). Furthermore, similar to *sakura* RNAi (**Fig 5**), *TOsk-Gal4*-driven *otu* RNAi knockdown did not affect ovary morphology (**Fig 11B**), but it did result in a reduced number of eggs laid and stage 14 oocytes compared with control RNAi (w^{RNAi}) (**Figure 11C** and **11D**).

When *sakura* and *otu* were independently RNAi-knockdowned in the germline driven by *UAS-Dcr2* and *NGT-Gal4*, the percentages of germless ovaries for *otu-RNAi* and *sakura-RNAi* were similar (~70%) (**Fig 8**). However, when *otu* and *sakura* were knocked down together, the percentage of germless ovaries increased significantly to 79% (**Fig 8**), suggesting that the double knockdown of *otu* and *sakura* enhances the germless phenotype in the ovaries.

Next, we used the *Burdock* sensor to test if loss of *otu* leads to loss of piRNA-mediated transposon silencing in the germline. Similar to *sakura* (**Fig 4D**), germline depletion of *otu* resulted in elevated GFP and β-Gal produced by the *Burdock* sensor (**Fig 11E**), indicating loss of piRNA-mediated transposon silencing. To determine if germ cell loss caused by *otu-RNAi* is a result of apoptosis, we stained the rudimentary ovaries of *otu-RNAi* for cleaved Caspase-3. Similar to $sakura^{null/null}$ (**Fig 3B**), cleaved Caspase-3 signals were higher in *otu-RNAi* ovaries than in controls, suggesting that the observed germ cell loss is due to apoptosis (**Fig 11F**).

Loss of *sakura* leads to misexpression of *bam*, likely due to low levels of pMad in the germ cells (**Fig 7A-C**). We were curious whether a similar occurrence could be observed in *otu-RNAi*. In the *otu* germline RNAi knockdown ovaries, we found that Bam-GFP expression is not restricted to the germarium but persists throughout the ovariole, resulting in an excess number of Bam-GFP-positive cells (**Fig 12A**). We also observed lower pMad levels in $otu^{14/14}$ mutant GSCs (**Fig 12B**). These data suggest that, similar to *sakura*, loss of *otu* results in *bam* derepression, likely due to low levels of pMad in the germ cells.

A previous study has shown that Otu possesses deubiquitinase activity[21]. We asked whether Sakura regulates the Otu's deubiquitinase activity. To test this, we performed an in vitro deubiquitination assay using Ub-Rhodamine 110 as a model substrate. Consistent with previous studies[21], we detected a deubiquitinase activity in Otu that was ectopically expressed and purified from S2 cells (**Fig S6**). The presence of Sakura, purified from *E.coli*, did not affect Otu's deubiquitinase activity under these assay conditions. Additionally, Sakura itself did not exhibit deubiquitinase activity.

Taken together, these findings show that *otu* and *sakura* phenocopy each other in ovaries, specifically in regulating germ cell maintenance and differentiation, raising the possibility that they function together. Similar to *sakura*, loss of *otu* inhibits Dpp/BMP signaling and results in the de-repression of bam, leading to aberrant germline differentiation.

Discussion

In this study, we identified Sakura, encoded by a previously uncharacterized gene *CG14545*, as an essential factor for oogenesis and female fertility. We demonstrated that Sakura is specifically expressed in germline cells in the ovary, including GSCs, is localized to the cytoplasm, and is enriched in the developing oocytes. *sakura* homozygous null mutant flies are viable but completely female-sterile and male-fertile. Loss of *sakura*, either through null mutation or germline RNAi including in GSCs, results in rudimentary ovaries exhibiting germless and tumorous phenotypes.

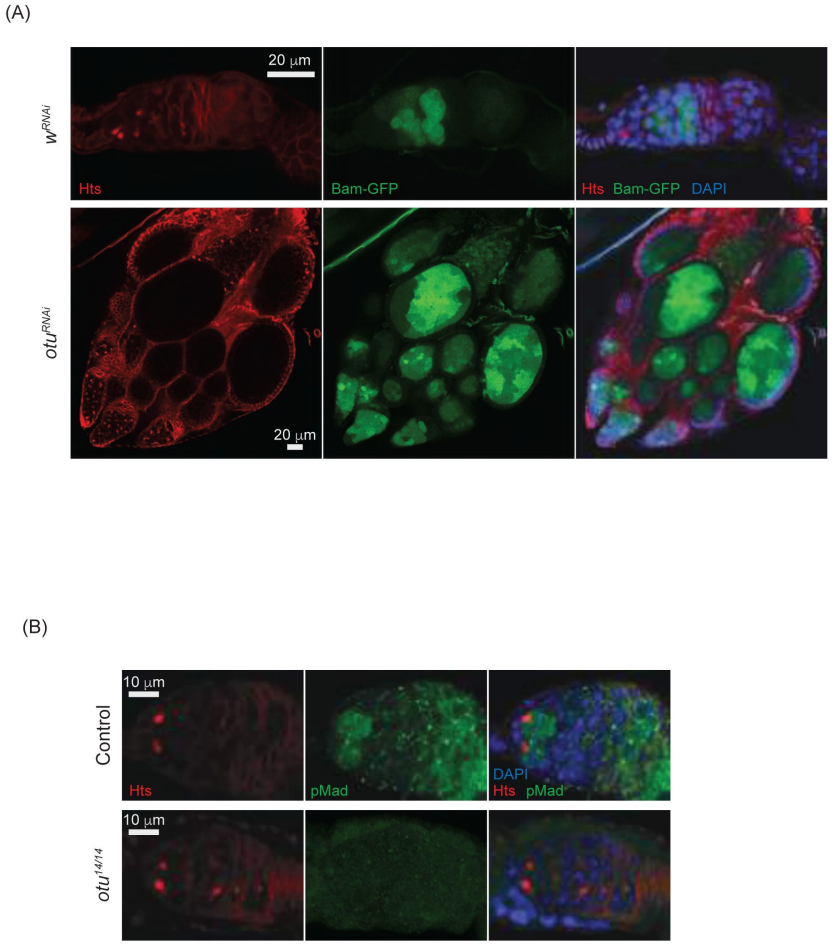

Fig 12.

Loss of *otu* results in low levels of pMad and derepression of *bam* in the germaria

(A) Confocal images of the ovaries from control (w^{RNAi}) and otu^{RNAi} flies harboring the *bam-GFP* reporter, where RNAi knockdown was driven in the female germline with *nos-Gal4-VP16*. Bam-GFP (green), Hts (red), and DAPI (blue). Scale bar: 20 μm. (B) Confocal images of germaria from control ($otu^{14/+}$) and $otu^{14/14}$ mutant flies stained with anti-pMad (green) and anti-Hts (red) antibodies. Scale bar: 10 μm.

The tumorous phenotype associated with the loss of *sakura* is characterized by an excess of GSC-like cells, which feature round spectrosomes, as well as cyst cells with branched fusomes (**Fig 3C**). The increased number of GSC-like cells in loss of *sakura* suggests dysregulation of GSC self-renewal and differentiation. Meanwhile, the presence of excess cyst cells with branched fusomes indicates abnormal differentiation and division of cysts. Differentiation of cystoblasts typically involves four mitotic divisions with incomplete cytokinesis, leading to 16 cyst cells interconnected by branched fusomes[7,46]. The degree of fusome branching serves as a marker for the stages of cyst cell division, with increased branching from 2-cell to 16-cell cysts[47–49]. Notably, fusomes begin to degenerate and disappear after 16-cell cysts as the germline cyst enters the meiotic zone or region 2 of the germarium[50,51]. The persistence of cyst cells with branched fusomes in $sakura^{null/null}$ suggests that *sakura* is crucial for the proper division and differentiation of cysts, and we speculate that it is required for germline cysts to enter meiotic division.

Mosaic analysis of $sakura^{null}$ indicates that *sakura* is intrinsically required for establishing GSCs in the ovaries. A significantly reduced number of $sakura^{null}$ marked GSCs were observed at the adult stage when mutant clones were induced in PGC stages, suggesting that many *sakura* mutant PGCs die before developing into GSCs. Furthermore, after inducing $sakura^{null}$ clones in adult ovaries, the number of marked $sakura^{null}$ GSCs decreased at a higher rate than controls, indicating a rapid loss of $sakura^{null}$ GSCs (**Fig 6A**). Thus, *sakura* is also intrinsically necessary for maintaining GSCs. Additionally, germaria containing $sakura^{null}$ GSCs became increasingly tumorous over time, with a growing number of $sakura^{null}$ GSC-like cells (**Fig 6B** and **6C**). This suggests that $sakura^{null}$ GSCs undergo uncontrolled division, becoming more tumorous over time, which eventually triggers an intrinsic cell death mechanism, as evidenced by elevated levels of cleaved Caspase-3 in $sakura^{null}$ ovaries (**Fig 3B**).

Dpp/BMP signaling governs GSC self-renewal and cystoblast differentiation by repressing *bam* in GSCs and de-repressing it in daughter cystoblasts (**Fig S1**). This process is mediated by the transcription factor Mad, which, when phosphorylated (pMad), translocates into the nucleus to repress *bam* transcription[7,46,52]. Our findings indicate that Bam expression is not limited to 8-cell cysts but continues throughout the germarium in ovaries lacking *sakura* function (**Fig 7A** and **7B**). The persistent expression of Bam is likely due to low levels of pMad in GSCs (**Fig 7C**, and 7D). Given the low pMad levels observed upon loss of *sakura*, we believe that the misregulation of Bam expression occurs primarily at the transcriptional level, although it has also been reported that Bam expression can be regulated post-transcriptionally[53].

Transposons are mobile genetic elements that, if not silenced, can generate DNA damage and genomic instability[54]. piRNAs derived from transposons and other repeats can target and silence transposon RNAs to preserve genome integrity in germ cells[31]. Loss of piRNAs leads to transposon derepression, resulting in increased DNA damage, which subsequently triggers cell death[55,56]. Genetic damage in germ cells can cause developmental defects and diseases that may be inherited by the next generation. Thus, elimination of defective germ cells is crucial for maintaining germline integrity of a species[57,58]. We found that loss of *sakura* results in reduced piRNA levels and loss of piRNA-mediated transposon silencing in the germline (**Fig 4**). The observed apoptosis, indicated by elevated cleaved Caspase-3 levels in *sakura* mutant ovaries (**Fig 3B**), suggest that desilencing of transposon due to reduced piRNA levels likely results in increased DNA damage, triggering cell death. We speculate that the germless phenotype in *sakura* mutants may partly arise from an apoptotic germline elimination program activated to maintain germline integrity. Loss of *piwi*, a key component of the piRNA pathway, similarly causes GSC-like tumors, as well as reduced *bam* expression and elevated pMad expression[29]. While downregulation of *bam* and upregulation of pMad in *piwi* mutant is opposite to upregulation of *bam* and downregulation of pMad in *sakura* mutant, defects in the piRNA pathway might be a shared underlying cause for the dysregulation of *bam* and pMad levels in both cases, leading to tumorous phenotype.

In addition to its expression in GSCs and cysts in the germarium, Sakura is also expressed in germline cells in later-stage egg chambers (**Fig 1E-F**) and is required at this stage for proper oogenesis. When Sakura is depleted from region 2b of the germarium onward, while leaving GSCs and early cyst cells intact, female flies lay significantly fewer eggs and have fewer stage 14 oocytes (**Fig 5**). The failure to produce stage 14 oocytes likely results from the Orb mislocalization in developing oocytes (**Fig 5E**). Orb is an RNA-binding protein crucial for egg chamber formation, oocyte specification, and polarity establishment during oogenesis by regulating mRNA localization and translation, such as that of *oskar*, which is vital for establishing oocyte anterior-posterior polarity[34,59]. Interestingly, piRNA pathway mutants exhibit Orb mislocalization in developing oocytes[60]. Therefore, reduced piRNA levels observed (**Fig 4**) may underlie the Orb mislocalization in loss of *sakura* (**Fig 5E**).

Sakura does not possess any known protein domains, complicating investigations into its molecular function. To infer its function, we identified interacting proteins through immunoprecipitation followed by mass spectrometry. We identified Otu, a protein known to be crucial for oogenesis, as a protein partner of Sakura. Mutations in *otu* gene lead to a range of ovarian phenotypes, including germ cell loss, tumorous egg chambers filled with undifferentiated germ cells, abnormalities in nurse cell chromosome structure, and defects in oocyte determination[22,23]. We showed that germline depletion of Otu via RNAi phenocopies loss of *sakura*. Similar to Sakura, loss of *otu* inhibits Dpp/BMP signaling, resulting in low pMad levels in GSCs and Bam de-repression (**Fig 12A-B**). Additionally, loss of *otu* also results in the loss of piRNA-mediated silencing, paralleling the effects of *sakura* loss. Furthermore, germline knockdown of *otu* yielded a similar ratio of germless ovaries as seen in *sakura-RNAi,* and simultaneous knockdown of both *otu* and *sakura* exacerbated the germless ovary phenotype (**Fig 8**). These observations raise the possibility that Sakura and Otu function together to regulate germ cell maintenance in the ovaries and are involved in Dpp/BMP signaling to balance stem cell renewal and differentiation.

Otu possesses deubiquitinase activity, catalyzed by its N-terminal Otu domain[21,61]. In germ cells, Otu interacts with Bam, forming a deubiquitinase complex that deubiquitinates and thereby stabilizes CycA, promoting GSC differentiation[21]. The predicted structure of Sakura and Otu complex suggests that the Mid domain of Sakura directly contacts the Otu domain of Otu (**Fig 10A**). We found that Sakura lacks a deubiquitinase activity and it does not directly affect Otu's deubiquitinase rate in our in vitro assays using Ub-Rhodamine 110 as a substrate (**Fig S6**). This does not preclude the possibility that Sakura may still influence Otu's deubiquitinase activity, potentially guiding Otu to its substrate and determining substrate specificity. Our in vitro assays may not have detected such specificity changes. Otu is also an RNA-binding protein, and its deubiquitinase activity can be enhanced by bound RNAs[7]. Future studies should explore whether Sakura regulates Otu's RNA-binding or other RNA-related functions. Notably, while Otu is expressed in various tissues, including testes and gut[42,61], Sakura is exclusively expressed in ovaries, particularly in germline cells such as GSCs, Therefore, Sakura may enhance Otu's functions specific to female germline cells. We believe that identifying Otu's deubiquitinase substrates and its RNA partners, along with investigating Sakura's role in these processes, will deepen our understanding of Sakura's and Otu's molecular functions in oogenesis. One speculative hypothesis is that Sakura may regulate Otu's deubiquitinase activity concerning piRNA pathway proteins crucial for proper piRNA production and function.

In summary, this study identifies and characterizes the previously unknown gene *sakura*, which is specifically expressed in female germ cells and is essential for oogenesis and female fertility. Together with its protein partner Otu, Sakura likely regulates germline cell fate, maintenance, and differentiation

Materials and methods

Fly strains

We generated the *sakura*^{null} strain by introducing indels within the Sakura coding region using the CRISPR/Cas9 genome editing system, as we previously reported[26,62–65]. The transgenic *sakura-EGFP, otu-EGFP,* and *otu(Δ-Tudor)-EGFP* strains were created following previously published methods[65,66]. A fragment containing Sakura cDNA flanked by ~1 kbp upstream and ~1 kbp downstream genomic sequences was cloned. Fragments containing Otu and Otu(Δ-Tudor) cDNAs, flanked by ~2.5 kbp upstream and ~1 kbp downstream genomic sequences, were also cloned. The EGFP gene was fused in-frame to the C-terminus of the Sakura and Otu coding sequences within these fragments, which were then inserted into a pattB plasmid vector. The *sakura-EGFP* plasmid was integrated into the 51C1 site within the fly genome using the BDSC:24482 fly strain and the PhiC31 system, while the *otu-EGFP* and *otu(Δ-Tudor)-EGFP* plasmids were integrated into the 25C6 site of the genome using the attP40 fly strain and the PhiC31 system.

The *sakura RNAi* #1 (VDRC: v39727) and #2 (VDRC: v103660), *y-RNAi* (v106068), *TOsk-Gal4* (v 314033), Burdock sensor [*UAS-Dcr2; NGT-Gal4; nosGal4-VP16, nos>NLS_GFP_lacZ_vas-3'UTR_burdock-target*] (v 313217) strains were from Vienna *Drosophila* Resource Center. *w-RNAi* (BDSC: 35573), *otu-RNAi* (BDSC: 34065), *bam-RNAi* (BDSC: 33631), *cycA-RNAi* (BDSC: 29313), *UAS-Dcr-2; NGT-Gal4* (BDSC: 25751), *FRT82B/TM6C, Sb* (BDSC: 86313) and *otu*[14] (BDSC: 6025) were obtained from the Bloomington Stock Center. The *bam-GFP* reporter (DGRC: 118177) and *vasa-EGFP* knocked-in fly (DGRC: 118616) were from Kyoto *Drosophila* Stock Center.

Fertility assay

The female fertility assay was performed as previously described[64,65,67,68]. Briefly, five test virgin females of each test genotype were mated with three wild-type (OregonR) males in a cage with a 6-cm grape juice agar plate supplemented with wet yeast paste. The agar plates were replaced daily, and the number of eggs laid on the third plate (on day 3) was recorded. After incubation at 25°C for an additional day, the number of hatched eggs was counted. At least three cages per genotype were tested.

For the male fertility assay, a single test male was mated with five wild-type (OregonR) virgin females in each vial, following previously published methods[64,65,67]. After 3 days, the females were transferred to a new vial (vial 1). Every two days, they were transferred to a new vial until a total of four vials were obtained. After 2 days in the fourth vial, the females were removed, and the total number of progenies emerging from these four vials was counted. At least five males per genotype were tested.

Sakura and Otu antibodies

We expressed a recombinant full-length Sakura protein as an N-terminal 6xHis-tagged protein in *E. coli* using a modified pET vector and purified it using Ni-sepharose (GE Healthcare) and HiTrapQ HP (GE Healthcare) columns, as we previously performed for other proteins[64,65]. Recombinant Otu fragments (145-405aa and 406-853aa) were similarly expressed as N-terminally 6xHis-MBP-fusion proteins in *E. coli* and purified using Ni-sepharose. These purified proteins were used as antigens to generate polyclonal anti-Sakura and anti-Otu sera in rabbits (Pocono Rabbit Farm & Laboratory, Inc.). The rabbit polyclonal anti-Sakura antibodies were affinity purified using His-MBP-Sakura recombinant protein and Affigel-15 (Bio-rad), following the manufacturer's instructions. Rabbit anti-Otu sera were first pre-cleared with purified His-MBP protein bound to Affigel-15, and the unbound fraction was affinity purified using purified His-MBP-Otu fragments (145-405aa and 406-853aa) and Affigel-15.

Germline clonal analysis

We generated *sakura*^{null} mutant clones using FLP/FRT-mediated recombination[69]. To create *sakura*^{null}GSC clones, 3-day-old female flies with the genotype *hs-flp*; +*; FRT82B, ubi-GFP/FRT82B, sakura*^{null} were heat-shocked at 37°C for 1 hour, twice daily, with an 8-hour interval between heat shocks. Female flies with the genotype *hs-flp*; +; *FRT82B, ubi-GFP/FRT82B* were used as controls. Flies were dissected and stained 4, 7, and 14 days after clone induction. To induce primordial germ cell (PGC) clones, early third-instar larvae were heat-shocked similarly, allowed to develop, and dissected and analyzed at 3 to 4 days post-eclosion.

Immunostaining

Stereomicroscope images of dissected ovaries were taken using Leica M125 stereomicrocsope[64]. Ovaries from 2- to 5-day-old, yeast-fed females were hand-dissected in 1X PBS (137 mM NaCl, 2.7 mM KCl, 10 mM Na_2HPO_4, 1.8 mM KH_2PO_4, pH 7.4) at room temperature. The dissected ovaries were fixed in a fixative buffer (4% formaldehyde, 15 mM PIPES (pH 7.0), 80 mM KCl, 20 mM NaCl2, 2 mM EDTA, and 0.5 mM EGTA), incubated for 30 minutes at room temperature with gentle rocking. After fixation, the ovaries were rinsed three times with PBX (0.1% Triton X-100 in 1X PBS) and then incubated in a blocking buffer (2% donkey serum in 3% BSA [w/v], 0.02% NAN3 [w/v] in PBX) for 1 hour at room temperature. Then, the ovaries were incubated with primary antibodies diluted in the blocking buffer overnight at 4°C. The following day, the ovaries were rinsed three times with PBX and incubated with Alexa Fluor-conjugated secondary antibodies for 2 hours. The ovaries were rinsed three times with PBX and then mounted in VECTASHIELD® PLUS antifade mounting medium with DAPI (H-2000, Vector lab). Confocal images were acquired on a Zeiss LSM700 confocal microscope at the Johns Hopkins University School of Medicine Microscope Facility.

The primary antibodies used for immunostaining were mouse anti-HTS (1B1) (DSHB, AB_528070, 1/100), mouse anti-Bam (DSHB, AB_10570327, 1/20), mouse anti-CycA (DSHB, AB_528188, 1/100), rat anti-Vasa (DSHB, AB_760351, 1/100), rabbit anti-pMad (Phospho-SMAD1/5 (Ser463/465) mAb #9516, dilution: 1/200, Cell Signaling), and rabbit anti-cleaved caspase-3 (Cleaved Caspase-3 (Asp175) #9661, dilution: 1/200, Cell Signaling). Secondary antibodies used were Alexa Fluor 488 Donkey anti-Mouse Igg (ThermoFisher A21202, 1/100), Alexa Fluor 594 Donkey anti-Rat Igg (ThermoFisher A21209, 1/100), Alexa Fluor 594 Donkey anti-Mouse Igg (ThermoFisher A21203, 1/100), and Alexa Fluor 594 Donkey anti-Rabbit Igg ThermoFisher A21207, 1/100).

Western blot

Lysates of hand-dissected ovaries and tissues were prepared by homogenizing in RIPA buffer (50 mM Tris-HCl [pH 7.4], 150 mM NaCl, 1% [v/v] IGEPAL CA-630, 0.1% [w/v] sodium dodecyl sulfate (SDS), 0.5% [w/v] sodium deoxycholate, 1 mM ethylenediaminetetraacetic acid (EDTA), 5 mM dithiothreitol, and 0.5 mM phenylmethylsulfonyl fluoride (PMSF))[63–65,67]. The homogenates were centrifuged at 21,000g at 4°C for 10 min, and the protein concentration of the supernatant was determined using the BCA protein assay kit (Pierce) as needed. Fifteen µg of total protein was loaded per lane for Western blot. The sources and dilutions of the primary antibodies were as below. Rabbit anti-Sakura (1/10000, generated in this study), rabbit anti-Otu (1/10000, generated in this study), rabbit anti-alpha-Tubulin [EP1332Y] (1/10000, Abcam, ab52866), mouse anti-alpha-Tubulin [12G10] (1/10000, DSHB, AB_1157911), mouse anti-FLAG (1/10000, Sigma, F1804), mouse anti-HA (1/10000, Sigma, H3663), and mouse anti-GFP [GF28R] (1/3000, Invitrogen, 14-6674-82). IRDye 800CW goat anti-mouse IgG, IRDye 800CW goat anti-rabbit IgG, IRDye 680RD goat anti-mouse, and IgG IRDye 680RD goat anti-rabbit were used as secondary antibodies. The membranes were scanned using the Li-Cor Odyssey CLx Imaging System.

Mass spectrometry

Immunoprecipitation of Sakura-EGFP protein was performed using the GFP-Trap Magnetic Agarose Kit (Proteintech, gtmak-20) on dissected ovaries from flies harboring *sakura-EGFP* transgene, with *w1118* flies as controls. Ovaries were homogenized in 200 µL ice-cold lysis buffer (10 mM Tris-HCl [pH 7.5], 150 mM NaCl, 0.5 mM EDTA, 0.05% [v/v] IGEPAL CA-630) containing 1× protease inhibitor cocktail (100× protease inhibitor cocktail contains 120 mg/ml 1 mM 4-(2-aminoethyl) benzene sulfonyl fluoride hydrochloride (AEBSF), 1 mg/ml aprotinin, 7 mg/ml bestatin, 1.8 mg/ml E-64, and 2.4 mg/ml leupeptin)[70]. After homogenization, the tubes were placed on ice for 30 minutes, and the homogenates were extensively pipetted every 10 minutes. The lysates were then centrifuged at 17,000x g for 10 minutes at 4°C. The supernatants were transferred to pre-chilled tubes, and 300 µL dilution buffer (10 mM Tris/Cl pH 7.5, 150 mM NaCl, 0.5 mM EDTA) supplemented with 1x protease inhibitor cocktail were added. The diluted lysates were then added to the GFP-trap magnetic beads in 1.5 mL tubes and rotated for 1 hour at 4°C. After separating the beads with a magnetic tube rack, the beads were washed three times with 500 µL wash buffer (10 mM Tris/Cl pH 7.5, 150 mM NaCl, 0.05 % [v/v] IGEPAL CA-630). Proteins were eluted with 40 µL acidic elution buffer (200 mM glycine pH 2.5) followed by immediate neutralization with 5 uL neutralization buffer (1 M Tris pH 10.4).

As a quality control before mass spectrometry, ~5 µL of the samples were mixed with an equal volume of 2× SDS-PAGE loading buffer (80 mM Tris-HCl [pH 6.8], 2% [w/v] SDS, 10% [v/v] glycerol, 0.0006% [w/v] bromophenol blue, 2% [v/v] 2-mercaptoethanol), heated at 95 °C for 3 min, and run on 4–20% Mini-PROTEAN® TGX™ Precast Protein Gels (Biorad, #4561094). Silver staining was then performed by using Pierce™ Silver Stain Kit (ThermoFisher, 24612) to assess the quality of the immunoprecipitated protein samples. Mass spectrometry was conducted at the Mass Spectrometry Core at the Department of Biological Chemistry, Johns Hopkins School of Medicine, as previously described[65]

Co-immunoprecipitation

For co-immunoprecipitation of endogenous Sakura protein, wild-type ovaries (*w1118*) were homogenized in RIPA buffer, centrifuged at 21,000g at 4°C for 10 min, and the clear supernatant protein lysates were used for immunoprecipitation. Four µg of rabbit anti-Sakura and normal rabbit IgG (Cell Signaling, #2729) were incubated with 50 µL of Dynabeads Protein G (ThermoFisher, 10004D) for 20 min at room temperature. The beads were washed once with PBST (1x PBS with 0.1% Tween-20). The ovary lysate supernatant was then incubated with the washed beads at room temperature for 30 min, followed by three washes with PBST. The proteins were eluted with 2x SDS-PAGE loading buffer (80 mM Tris-HCl [pH 6.8], 2% [w/v] SDS, 10% [v/v] glycerol, 0.0006% [w/v] bromophenol blue, 2% [v/v] 2-mercaptoethanol) and heated at 70°C for 10 min. After bead separation using a magnetic tube rack, the eluted proteins in 2x SDS-PAGE loading buffer were heated again at 95°C for 3 min.

Transient protein expression in S2 cells was performed using the pAc5.1/V5-HisB plasmid vector (Invitrogen). A total of 1 µg plasmids were transfected using the Effectene transfection reagent (Qiagen, 301425). Three days after transfection, cells were harvested and lysed with ice-cold lysis buffer supplemented with 1× protease inhibitor cocktail. The cell lysates were then centrifuged at 17,000x g for 10 min at 4°C, and the clear supernatants were collected for immunoprecipitation. For anti-HA immunoprecipitation, supernatants were incubated with 25 µL (0.25 mg) of Pierce™ Anti-HA Magnetic Beads (ThermoFisher, 88837) at room temperature for 30 min. The beads were then washed three times with TBST (1x TBS [0.05 M Tris/HCl and 0.15 M NaCl, pH 7.6] with 0.05% Tween-20). For anti-FLAG immunoprecipitation, 2 µg of mouse anti-FLAG (1/10000, Sigma, F1804) was incubated with 50 µL of Dynabeads Protein G (ThermoFisher, 10004D) for 10 min at room temperature. The beads were washed once with PBST. The S2 cell lysate supernatant was incubated with the washed beads at room temperature for 15 min. The beads were washed three

times with PBST. In both anti-HA and anti-FLAG immunoprecipitations, proteins were eluted with 2× SDS-PAGE loading buffer. For anti-HA, the beads in 2x SDS-PAGE loading buffer were heated at 95°C for 7 min. For anti-FLAG, the beads were heated at 70°C for 10 min, then were separated using a magnetic tube rack. The eluted proteins in 2x SDS-PAGE loading buffer were heated again at 95°C for 3 min.

Small RNA and mRNA sequencing

Poly-A+ mRNA purification was performed as previously described[71]. Small RNA libraries and poly-A+ mRNA libraries were prepared, sequenced on Hiseq2500 (Illumina), and analyzed, as previously reported[72,73]. SRA accession number for these datasets is PRJNA1156618.

In vitro deubiquitination assay

C-terminally 6xHis-tagged recombinant Sakura protein was expressed in *E. coli* using a modified pET vector and was purified using Ni-sepharose. N-terminally 3xHA-HRV3Csite-3xFLAG-tagged Otu protein and a negative control, N-terminally 3xHA-HRV3Csite-3xFLAG-tagged firefly luciferase protein, were expressed in S2 cells using pAc5.1/V5-HisB vector. The proteins were immunoprecipitated using Pierce™ Anti-HA Magnetic Beads (ThermoFisher, 88837) as described previously, with a more stringent washing step to effectively remove interacting proteins. The beads were washed six times with a high salt wash buffer (TBST with 800 mM NaCl). The proteins were eluted by cleaving off 3xHA tag with 25 nM GST-HRV3C protease in a cleavage buffer (25mM Tris-HCl pH 7.4, 150 mM NaCl, 5% glycerol, 2mM EDTA), incubated at 4°C with rotation for 6 hours. An equal volume of 100% glycerol was added to the eluted protein.

Purified proteins, including Otu, luciferase, and Sakura, were mixed with Ub-Rhodamine 110 (Ubiquitin-Proteasome Biotechnologies, M3020) in a total volume of 30 µL in reaction buffer (20 mM Tris-HCl, pH 7.5, 200 mM NaCl, 5 mM $MgCl_2$, 2 mM DTT). The mixture was added to a black 384-well low-volume plate. Fluorescence measurements were taken using SpectraMax i3x Multi-Mode Microplate Reader at 37°C, with excitation and emission wavelengths set at 485/20 and 530/20 nm respectively. The fluorescence intensity for each condition was averaged from triplicates and plotted as a function of time.

Acknowledgements

We thank Bloomington Drosophila Stock Center, Vienna Drosophila Resource Center, and Kyoto Drosophila Stock Center for fly strain stocks. We thank the Johns Hopkins University School of Medicine Microscope Facility for use of the Zeiss LSM700, supported by NIH grant S10OD016374 awarded to Dr. Scot C. Kuo. We thank Ms. Lauren DeVine and Dr. Bob Cole at the Johns Hopkins University School of Medicine Mass Spectrometry and Proteomics Core Facility for the mass-spec analysis. This work was supported by the grants from the National Institutes of Health [R35GM145352] and Johns Hopkins University Catalyst Award to RF.

Additional information

Author Contributions

Methodology and Investigation, A.A., L.Z., and R.F.; Conceptualization and Writing, A.A. and R.F.; Funding Acquisition and Supervision, R.F.

Competing interests

The authors have no conflicts of interest to declare.

Supplementary figures

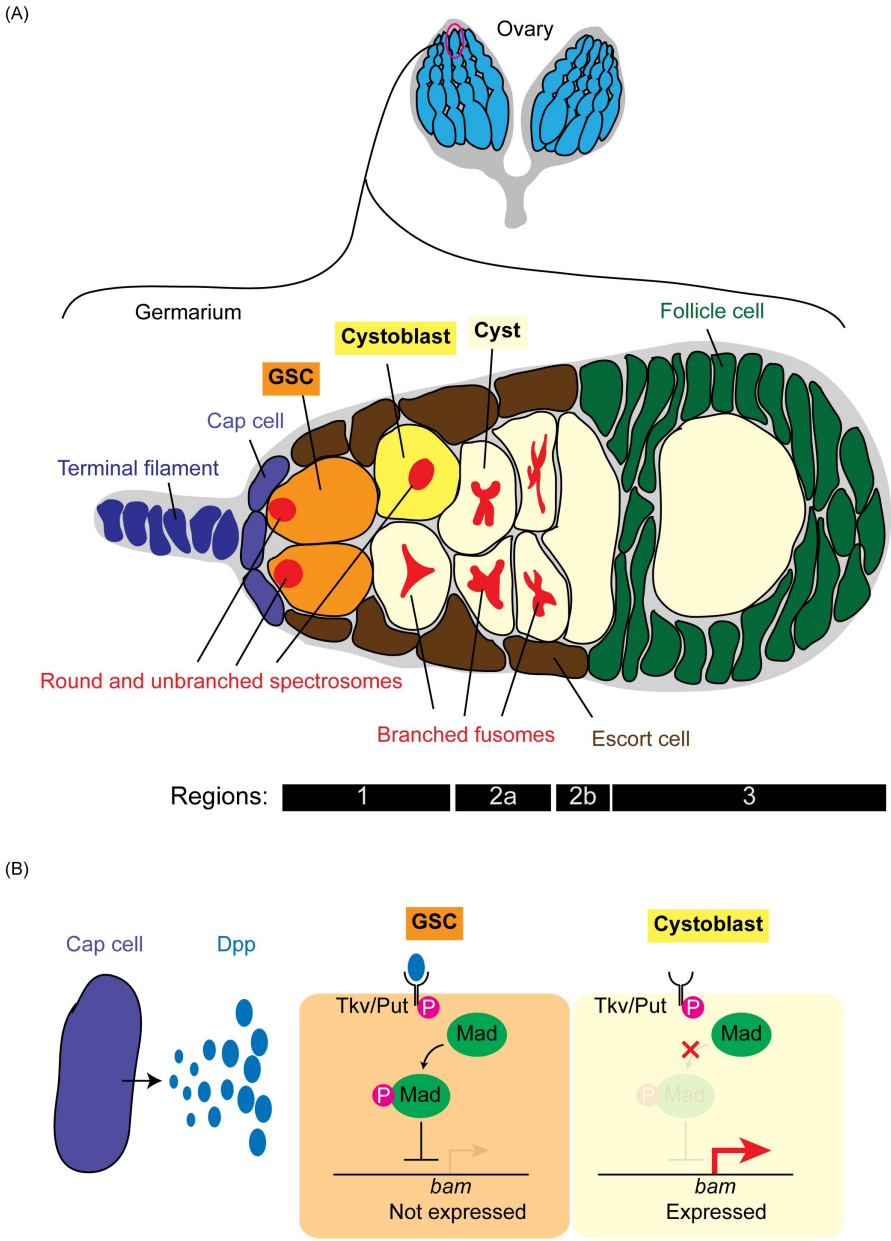

Fig S1.

Schematic illustration of Drosophila ovary and germarium

(A) Drosophila female has a pair of ovaries, each composed of 12-16 ovarioles. The germarium is located at the anterior tip of the ovarioles and consists of germ cells and somatic cells. Germline stem cells (GSCs), cystoblasts, cysts, and more differentiate oocytes are germ cells, while terminal filament cells, cap cells, escort cells, and follicle cells are somatic cells. GSCs and cystoblasts have round-shaped and unbranched spectrosomes, while cysts have branched fusomes. (B) Cap cells secrete diffusible Decapentaplegic (Dpp), which is received by its receptor, a heterodimer of Thick vein (Tkv) and Punt (Put), in GSCs. The activated Dpp signaling eventually phosphorylates Mother-against-dpp (Mad). The phosphorylated Mad (pMad) represses the transcription of *bag-of-marbles* (*bam*). The repression of *bam* in GSCs is crucial for maintaining their stemness. Cystoblasts do not receive Dpp, and Bam expression is crucial for promoting cystoblast differentiation from GSCs.

Fig S2.

Male fertility assay.

The numbers of the progeny flies obtained from crosses between test males and wild-type (OregonR) virgin females are shown. Mean ± SD (n = 5).

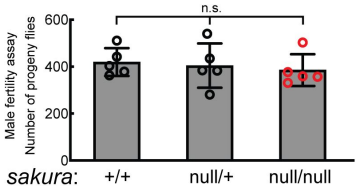

Fig S3.

sakura^{null} ovaries are tumorous

Violin plots of GSC-like cell numbers in germaria of indicated genotypes. Mean ± SD and the biological replicate number n are also shown. P-value < 0.05 (Student's t-test, unpaired, two-tailed) is indicated by *

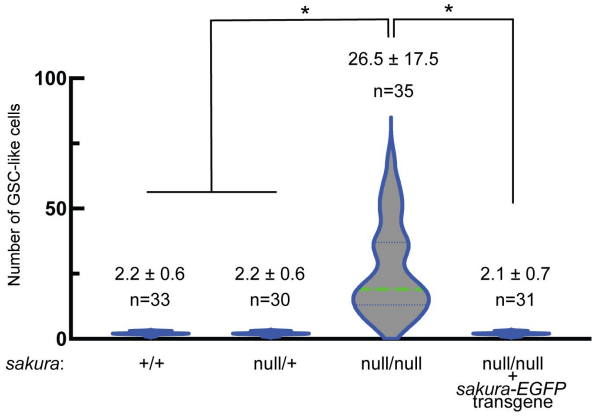

Fig S4.

sakura^{null} clone germline cells intrinsically cause tumorous phenotype

Violin plots of GSC-like cell number in germaria of indicated genotypes. Mean ± SD, and the biological replicated number n are also shown. P-value < 0.05 (Student's t-test, unpaired, two-tailed) are indicated by *

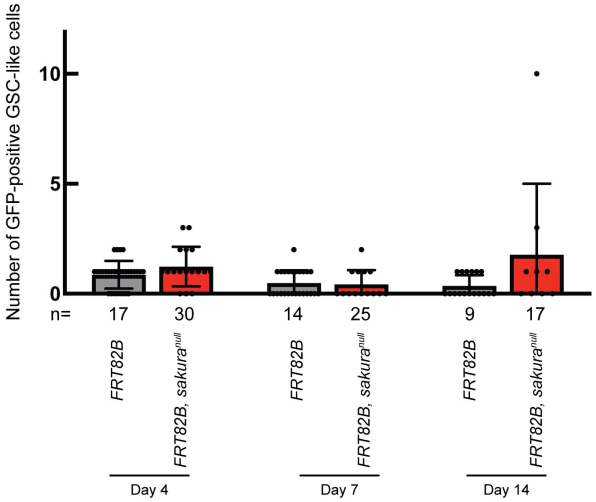

Fig S5.

Co-immunoprecipitations assay to test interaction between N-terminal fragments of Sakura and Otu in S2 cells

Co-immnuprocepitation assay using beads bound with anti-FLAG antibody followed by Western blotting. S2 cell lysates expressing mCherry-3xHA were used as controls. This is the reciprocal co-immunoprecipitation of **Fig 10F**.

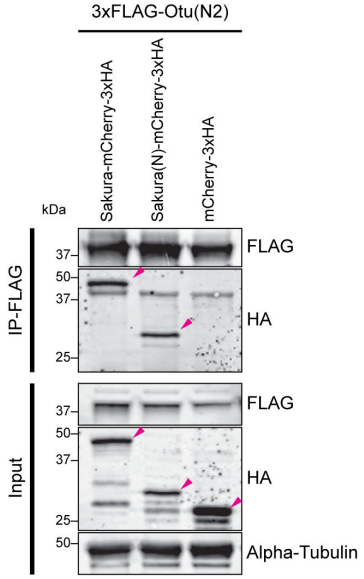

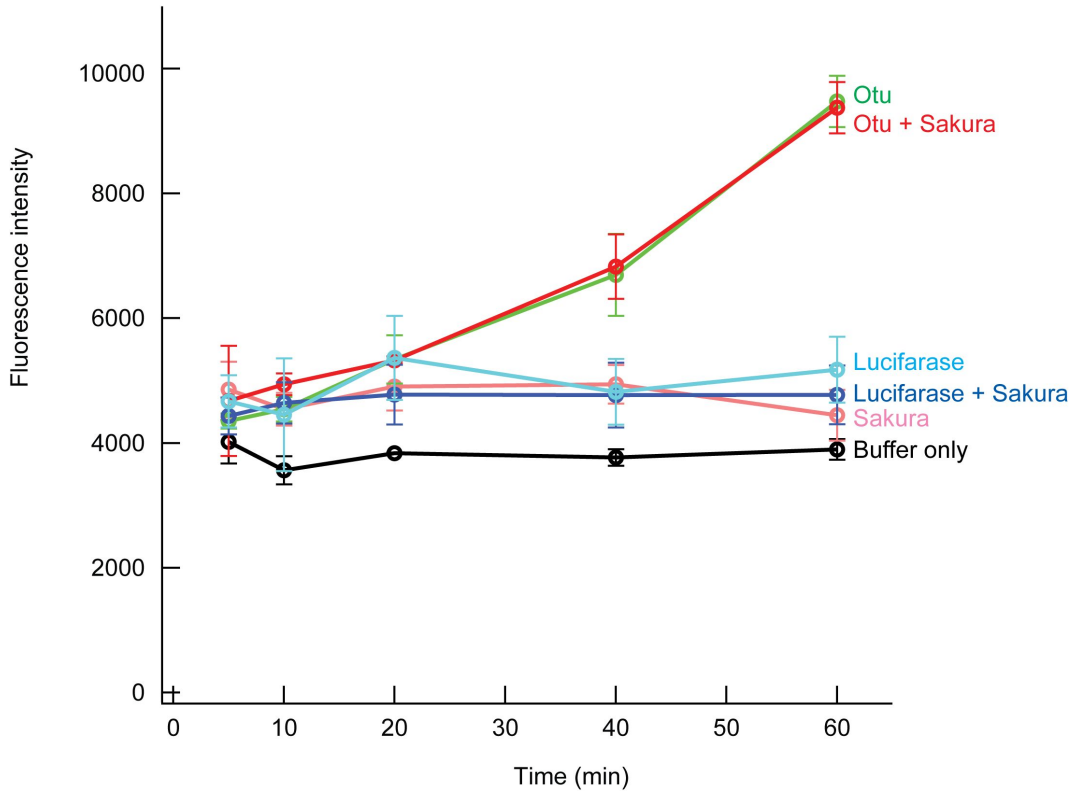

Fig S6.

In vitro deubiquitination assay.

The mean fluorescence intensity of three replicates was plotted. Error bars (+/-) are standard deviations. Firefly Luciferase was used as a negative control.

References

1. Lin H., Spradling A. C (1993) **Germline Stem Cell Division and Egg Chamber Development in Transplanted Drosophila Germaria** *Dev. Biol* **159**:140–152

2. de Cuevas M., Matunis E. L (2011) **The stem cell niche: lessons from the Drosophila testis** *Development* **138**:2861–2869

3. Losick V. P., Morris L. X., Fox D. T., Spradling A (2011) **Drosophila Stem Cell Niches: A Decade of Discovery Suggests a Unified View of Stem Cell Regulation** *Dev. Cell* **21**:159–171

4. Schüpbach T., Wieschaus E., Nöthiger R (1978) **A study of the female germ line in mosaics of Drosophila. Wilhelm Rouxs Arch** *Dev. Biol* **184**:41–56

5. Spradling A. C (1993) **Germline cysts: Communes that work** *Cell* **72**:649–651

6. Lin H., Yue L., Spradling A. C (1994) **The Drosophila fusome, a germline-specific organelle, contains membrane skeletal proteins and functions in cyst formation** *Development* **120**:947–956

7. Kirilly D., Xie T (2007) **The Drosophila ovary: an active stem cell community** *Cell Res* **17**:15–25

8. Lin H (1997) **The Tao of stem cells in the germline** *Annu. Rev. Genet* **31**:455–491

9. Cox D. N., et al. (1998) **A novel class of evolutionarily conserved genes defined by piwi are essential for stem cell self-renewal** *Genes Dev* **12**:3715–3727

10. Gateff E., et al. (1996) **Drosophila differentiation genes instrumental in tumor suppression** *Int. J. Dev. Biol* **40**:149–156

11. Ohlstein B., Lavoie C. A., Vef O., Gateff E., McKearin D. M (2000) **The Drosophila cystoblast differentiation factor, benign gonial cell neoplasm, is related to DExH-box proteins and interacts genetically with bag-of-marbles** *Genetics* **155**:1809–1819

12. Song X., Zhu C.-H., Doan C., Xie T (2002) **Germline Stem Cells Anchored by Adherens Junctions in the Drosophila Ovary Niches** *Science* **296**:1855–1857

13. Gilboa L., Forbes A., Tazuke S. I., Fuller M. T., Lehmann R (2003) **Germ line stem cell differentiation in Drosophila requires gap junctions and proceeds via an intermediate state** *Development* **130**:6625–6634

14. Xie T., Spradling A (1998) **C. decapentaplegic Is Essential for the Maintenance and Division of Germline Stem Cells in the Drosophila Ovary** *Cell* **94**:251–260

15. Casanueva M. O., Ferguson E. L (2004) **Germline stem cell number in the Drosophila ovary is regulated by redundant mechanisms that control Dpp signaling** *Development* **131**:1881–1890

16. Kai T., Spradling A (2003) **An empty Drosophila stem cell niche reactivates the proliferation of ectopic cells** *Proc. Natl. Acad. Sci* **100**:4633–4638

17. Song X., et al. (2004) **Bmp signals from niche cells directly repress transcription of a differentiation-promoting gene, bag of marbles, in germline stem cells in the Drosophila ovary** *Development* **131**:1353–1364

18. McKearin D. M., Spradling A (1990) **C. bag-of-marbles: a Drosophila gene required to initiate both male and female gametogenesis** *Genes Dev* **4**:2242–2251

19. Ohlstein B., McKearin D (1997) **Ectopic expression of the Drosophila Bam protein eliminates oogenic germline stem cells** *Development* **124**:3651–3662

20. McKearin D., Ohlstein B (1995) **A role for the Drosophila Bag-of-marbles protein in the differentiation of cystoblasts from germline stem cells** *Development* **121**:2937–2947

21. Ji S., et al. (2017) **Bam-dependent deubiquitinase complex can disrupt germ-line stem cell maintenance by targeting cyclin A** *Proc. Natl. Acad. Sci* **114**:6316–6321

22. King R. C., Riley S. F (1982) **Ovarian pathologies generated by various alleles of the otu locus in Drosophila melanogaster** *Dev. Genet* **3**:69–89

23. Glenn L. E., Searles L. L (2001) **Distinct domains mediate the early and late functions of the Drosophila ovarian tumor proteins** *Mech. Dev* **102**:181–191

24. Storto P. D., King R. C (1988) **Multiplicity of functions for the otu gene products during Drosophila oogenesis** *Dev. Genet* **9**:91–120

25. Rodesch C., Pettus J., Nagoshi R. N (1997) **The Drosophila ovarian tumor Gene Is Required for the Organization of Actin Filaments during Multiple Stages in Oogenesis** *Dev. Biol* **190**:153–164

26. Kondo S., Ueda R (2013) **Highly Improved Gene Targeting by Germline-Specific Cas9 Expression in Drosophila** *Genetics* **195**:715–721

27. Yang F., et al. (2019) **Ovaries absent links dLsd1 to HP1a for local H3K4 demethylation required for heterochromatic gene silencing** *eLife* **8**

28. Eliazer S., Shalaby N. A., Buszczak M (2011) **Loss of lysine-specific demethylase 1 nonautonomously causes stem cell tumors in the Drosophila ovary** *Proc. Natl. Acad. Sci* **108**:7064–7069

29. Jin Z., Flynt A. S., Lai E. C (2013) **Drosophila piwi mutants exhibit germline stem cell tumors that are sustained by elevated Dpp signaling** *Curr. Biol. CB* **23**:1442–1448

30. Handler D., et al. (2013) **The Genetic Makeup of the Drosophila piRNA Pathway** *Mol. Cell* **50**:762–777

31. Siomi M. C., Sato K., Pezic D., Aravin A. A (2011) **PIWI-interacting small RNAs: the vanguard of genome defence** *Nat. Rev. Mol. Cell Biol* **12**:246–258

32. Dönertas D., Sienski G., Brennecke J (2013) **Drosophila Gtsf1 is an essential component of the Piwi-mediated transcriptional silencing complex** *Genes Dev* **27**:1693–1705

33. ElMaghraby M. F., Tirian L., Senti K.-A., Meixner K., Brennecke J (2021) **A genetic toolkit for studying transposon control in the Drosophila melanogaster ovary** *Genetics* **220**

34. Barr J., Gilmutdinov R., Wang L., Shidlovskii Y., Schedl P (2019) **The Drosophila CPEB Protein Orb Specifies Oocyte Fate by a 3UTR-Dependent Autoregulatory Loop** *Genetics* **213**:1431–1446

35. Xu T., Rubin G. M (1993) **Analysis of genetic mosaics in developing and adult Drosophila tissues** *Development* **117**:1223–1237

36. Yang L., et al. (2007) **Argonaute 1 regulates the fate of germline stem cells in Drosophila** *Development* **134**:4265–4272

37. Hayashi Y., Yoshinari Y., Kobayashi S., Niwa R (2020) **The regulation of Drosophila ovarian stem cell niches by signaling crosstalk** *Curr. Opin. Insect Sci* **37**:23–29

38. Chen D., McKearin D. M (2003) **A discrete transcriptional silencer in the bam gene determines asymmetric division of the Drosophila germline stem cell** *Development* **130**:1159–1170

39. Chen D., et al. (2009) **Effete-mediated degradation of Cyclin A is essential for the maintenance of germline stem cells in Drosophila** *Development* **136**:4133–4142

40. Chen D., McKearin D (2003) **Dpp Signaling Silences bam Transcription Directly to Establish Asymmetric Divisions of Germline Stem Cells** *Curr. Biol* **13**:1786–1791

41. Xia L., et al. (2010) **The Fused/Smurf Complex Controls the Fate of Drosophila Germline Stem Cells by Generating a Gradient BMP Response** *Cell* **143**:978–990

42. Steinhauer W. R., Kalfayan L. J (1992) **A specific ovarian tumor protein isoform is required for efficient differentiation of germ cells in Drosophila oogenesis** *Genes Dev* **6**:233–243

43. Buskirk C. V., Schüpbach T. (2002) **half pint Regulates Alternative Splice Site Selection in Drosophila** *Dev. Cell* **2**:343–353

44. Sass G. L., Comer A. R., Searles L. L (1995) **The Ovarian Tumor Protein Isoforms of Drosophila melanogaster Exhibit Differences in Function, Expression, and Localization** *Dev. Biol* **167**:201–212

45. Jumper J., et al. (2021) **Highly accurate protein structure prediction with AlphaFold** *Nature* **596**:583–589

46. Hinnant T. D., Merkle J. A., Ables E. T. (2020) **Coordinating Proliferation, Polarity, and Cell Fate in the Drosophila Female Germline** *Front. Cell Dev. Biol* **8**

47. Christophorou N., Rubin T., Huynh J.-R (2013) **Synaptonemal Complex Components Promote Centromere Pairing in Pre-meiotic Germ Cells** *PLoS Genet* **9**

48. Hinnant T. D., Alvarez A. A., Ables E. T (2017) **Temporal remodeling of the cell cycle accompanies differentiation in the Drosophila germline** *Dev. Biol* **429**:118–131

49. Mathieu J., Michel-Hissier P., Boucherit V., Huynh J.-R (2022) **The deubiquitinase USP8 targets ESCRT-III to promote incomplete cell division** *Science* https://doi.org/10.1126/science.abg2653

50. Cuevas M. de, Spradling A. C (1998) **Morphogenesis of the Drosophila fusome and its implications for oocyte specification** *Development* **125**:2781–2789

51. Snapp E. L., Iida T., Frescas D., Lippincott-Schwartz J., Lilly M. A (2004) **The Fusome Mediates Intercellular Endoplasmic Reticulum Connectivity in Drosophila Ovarian Cysts** *Mol. Biol. Cell* **15**:4512–4521

52. Kahney E. W., Snedeker J. C., Chen X (2019) **Regulation of Drosophila germline stem cells** *Curr. Opin. Cell Biol* **60**:27–35

53. Pek J. W., Lim A. K., Kai T (2009) **Drosophila Maelstrom Ensures Proper Germline Stem Cell Lineage Differentiation by Repressing microRNA-7** *Dev. Cell* **17**:417–424

54. Levin H. L., Moran J. V (2011) **Dynamic interactions between transposable elements and their hosts** *Nat. Rev. Genet* **12**:615–627

55. Moon S., et al. (2018) **A Robust Transposon-Endogenizing Response from Germline Stem Cells** *Dev. Cell* **47**:660–671

56. Kang I., et al. (2018) **Identification of target genes regulated by the Drosophila histone methyltransferase Eggless reveals a role of Decapentaplegic in apoptotic signaling** *Sci. Rep* **8**

57. Ota R., Kobayashi S (2020) **Myc plays an important role in Drosophila P-M hybrid dysgenesis to eliminate germline cells with genetic damage. Commun** *Biol* **3**:1–8

58. Chu H.-P., et al. (2014) **Germline Quality Control: eEF2K Stands Guard to Eliminate Defective Oocytes** *Dev. Cell* **28**:561–572

59. Chang J. S., Tan L., Schedl P (1999) **The Drosophila CPEB Homolog, Orb, Is Required for Oskar Protein Expression in Oocytes** *Dev. Biol* **215**:91–106

60. Ohtani H., et al. (2013) **DmGTSF1 is necessary for Piwi–piRISC-mediated transcriptional transposon silencing in the Drosophila ovary** *Genes Dev* **27**:1656–1661

61. Ji S., et al. (2019) **LC Domain-Mediated Coalescence Is Essential for Otu Enzymatic Activity to Extend Drosophila Lifespan** *Mol. Cell* **74**:363–377

62. Zhu L., Kandasamy S. K., Fukunaga R (2018) **Dicer partner protein tunes the length of miRNAs using base-mismatch in the pre-miRNA stem** *Nucleic Acids Res* **46**:3726–3741

63. Zhu L., Liao S. E., Fukunaga R (2019) **Drosophila Regnase-1 RNase is required for mRNA and miRNA profile remodelling during larva-to-adult metamorphosis** *RNA Biol* **16**:1386–1400

64. Zhu L., Kandasamy S. K., Liao S. E., Fukunaga R (2018) **LOTUS domain protein MARF1 binds CCR4-NOT deadenylase complex to post-transcriptionally regulate gene expression in oocytes** *Nat. Commun* **9**

65. Zhu L., Fukunaga R (2021) **RNA-binding protein Maca is crucial for gigantic male fertility factor gene expression, spermatogenesis, and male fertility, in Drosophila** *PLOS Genet* **17**

66. Fukunaga R., et al. (2012) **Dicer Partner Proteins Tune the Length of Mature miRNAs in Flies and Mammals** *Cell* **151**:533–546

67. Liao S. E., Kandasamy S. K., Zhu L., Fukunaga R (2019) **DEAD-box RNA helicase Belle posttranscriptionally promotes gene expression in an ATPase activity-dependent manner** *RNA* **25**:825–839

68. Zhu L., Liao S. E., Ai Y., Fukunaga R (2019) **RNA methyltransferase BCDIN3D is crucial for female fertility and miRNA and mRNA profiles in Drosophila ovaries** *PLOS One* **14**

69. Rubin T., Huynh J.-R (2015) **Mosaic Analysis in the Drosophila melanogaster Ovary** *Methods Mol. Biol. Clifton NJ* **1328**:29–55

70. Kandasamy S. K., Zhu L., Fukunaga R (2017) **The C-terminal dsRNA-binding domain of Drosophila Dicer-2 is crucial for efficient and high-fidelity production of siRNA and loading of siRNA to Argonaute2** *RNA* **23**:1139–1153

71. Wang L., et al. (2011) **A Low-Cost Library Construction Protocol and Data Analysis Pipeline for Illumina-Based Strand-Specific Multiplex RNA-Seq** *PLOS One* **6**

72. Han B. W., Wang W., Li C., Weng Z., Zamore P. D (2015) **piRNA-guided transposon cleavage initiates Zucchini-dependent, phased piRNA production** *Science* **348**:817–821

73. Zhang Z., Theurkauf W. E., Weng Z., Zamore P. D (2012) **Strand-specific libraries for high throughput RNA sequencing (RNA-Seq) prepared without poly(A) selection** *Silence* **3**

Author information

Azali Azlan
Department of Biological Chemistry, Johns Hopkins School of Medicine, Baltimore, United States

Li Zhu
Department of Biological Chemistry, Johns Hopkins School of Medicine, Baltimore, United States

Ryuya Fukunaga
Department of Biological Chemistry, Johns Hopkins School of Medicine, Baltimore, United States
ORCID iD: 0000-0002-5814-8206

For correspondence: fukunaga@jhmi.edu

Editors

Reviewing Editor
Olivia Rissland
University of Colorado School of Medicine, Aurora, United States of America

Senior Editor
Sofia Araújo
University of Barcelona, Barcelona, Spain

Reviewer #1 (Public review):

Summary:

In this manuscript, Azlan et al. identified a novel maternal factor called Sakura that is required for proper oogenesis in Drosophila. They showed that Sakura is specifically expressed in the female germline cells. Consistent with its expression pattern, Sakura functioned autonomously in germline cells to ensure proper oogenesis. In Sakura KO flies, germline cells were lost during early oogenesis and often became tumorous before degenerating by apoptosis. In these tumorous germ cells, piRNA production was defective and many transposons were derepressed. Interestingly, Smad signaling, a critical signaling pathway for GSC maintenance, was abolished in sakura KO germline stem cells, resulting in ectopic expression of Bam in whole germline cells in the tumorous germline. A recent study reported that Bam acts together with the deubiquitinase Otu to stabilize Cyc A. In the absence of sakura, Cyc A was upregulated in tumorous germline cells in the germarium. Furthermore, the authors showed that Sakura co-immunoprecipitated Otu in ovarian extracts. A series of in vitro assays suggested that the Otu (1-339 aa) and Sakura (1-49 aa) are sufficient for their direct interaction. Finally, the authors demonstrated that the loss of otu phenocopies the loss of sakura, supporting their idea that Sakura plays a role in germ cell maintenance and differentiation through interaction with Otu during oogenesis.

Strengths:

To my knowledge, this is the first characterization of the role of CG14545 genes. Each experiment seems to be well-designed and adequately controlled.

Weaknesses:

However, the conclusions from each experiment are somewhat separate, and the functional relationships between Sakura's functions are not well established. In other words, although the loss of Sakura in the germline causes pleiotropic effects, the cause-and-effect relationships between the individual defects remain unclear.

https://doi.org/10.7554/eLife.103828.1.sa2

Reviewer #2 (Public review):

In this study, the authors identified CG14545 (and named it Sakura), as a key gene essential for Drosophila oogenesis. Genetic analyses revealed that Sakura is vital for both oogenesis progression and ultimate female fertility, playing a central role in the renewal and differentiation of germ stem cells (GSC).

The absence of Sakura disrupts the Dpp/BMP signaling pathway, resulting in abnormal bam gene expression, which impairs GSC differentiation and leads to GSC loss. Additionally, Sakura is critical for maintaining normal levels of piRNAs. Also, the authors convincingly demonstrate that Sakura physically interacts with Otu, identifying the specific domains necessary for this interaction, suggesting a cooperative role in germline regulation. Importantly, the loss of otu produces similar defects to those observed in Sakura mutants, highlighting their functional collaboration.

The authors provide compelling evidence that Sakura is a critical regulator of germ cell fate, maintenance, and differentiation in Drosophila. This regulatory role is mediated through the modulation of pMad and Bam expression. However, the phenotypes observed in the germarium appear to stem from reduced pMad levels, which subsequently trigger premature and ectopic expression of Bam. This aberrant Bam expression could lead to increased CycA levels and altered transcriptional regulation, impacting piRNA expression. Given Sakura's role in pMad expression, it would be insightful to investigate whether overexpression of Mad or pMad could mitigate these phenotypic defects (UAS-Mad line is available at Bloomington Drosophila Stock Center).

A major concern is the overstated role of Sakura in regulating Orb. The data does not reveal mislocalized Orb; rather, a mislocalized oocyte and cytoskeletal breakdown, which may be secondary consequences of defects in oocyte polarity and structure rather than direct misregulation of Orb. The conclusion that Sakura is necessary for Orb localization is not supported by the data. Orb still localizes to the oocyte until about stage 6. In the later stage, it looks like the cytoskeleton is broken down and the oocyte is not positioned properly, however, there is still Orb localization in the ~8-stage egg chamber in the oocyte. This phenotype points towards a defect in the transport of Orb and possibly all other factors that need to localize to the oocyte due to cytoskeletal breakdown, not Orb regulation directly. While this result is very interesting it needs further evaluation on the underlying mechanism. For example, the decrease in E-cadherin levels leads to a similar phenotype and Bam is known to regulate E-cadherin expression. Is Bam expressed in these later knockdowns?

The manuscript would benefit from a more balanced interpretation of the data concerning Sakura's role in Orb regulation. Furthermore, a more expanded discussion on Sakura's potential role in pMad regulation is needed. For example, since Otu and Bam are involved in translational regulation, do the authors think that Mad is not translated and therefore it is the reason for less pMad? Currently the discussion presents just a summary of the results and not an extension of possible interpretation discussed in context of present literature.

https://doi.org/10.7554/eLife.103828.1.sa1

Reviewer #3 (Public review):

In this very thorough study, the authors characterize the function of a novel Drosophila gene, which they name Sakura. They start with the observation that sakura expression is predicted to be highly enriched in the ovary and they generate an anti-sakura antibody, a line with a GFP-tagged sakura transgene, and a sakura null allele to investigate sakura localization and function directly. They confirm the prediction that it is primarily expressed in the ovary and, specifically, that it is expressed in germ cells, and find that about 2/3 of the mutants lack germ cells completely and the remaining have tumorous ovaries. Further investigation reveals that Sakura is required for piRNA-mediated repression of transposons in germ cells. They also find evidence that sakura is important for germ cell specification during development and germline stem cell maintenance during adulthood. However, despite the role of sakura in maintaining germline stem cells, they find that sakura mutant germ cells also fail to differentiate properly such that mutant germline stem cell clones have an increased number of "GSC-like" cells. They attribute this phenotype to a failure in the repression of Bam by dpp signaling. Lastly, they demonstrate that sakura physically interacts with otu and that sakura and otu mutants have similar germ cell phenotypes. Overall, this study helps to advance the field by providing a characterization of a novel gene that is required for oogenesis. The data are generally high-quality and the new lines and reagents they generated will be useful for the field. However, there are some weaknesses and I would recommend that they address the comments in the Recommendations for the authors section below.

https://doi.org/10.7554/eLife.103828.1.sa0